Bejan's Heatlines and Masslines for Convection Visualization and Analysis

V. A. F. Costa
Departamento de Engenharia Mecânica da
Universidade de Aveiro,
Campus Universitário de Santiago,
3810-193 Aveiro, Portugal
e-mail: v_costa@mec.ua.pt

Heatlines were proposed in 1983 by Kimura and Bejan (1983) as adequate tools for visualization and analysis of convection heat transfer. The masslines, their equivalent to apply to convection mass transfer, were proposed in 1987 by Trevisan and Bejan. These visualization and analysis tools proved to be useful, and their application in the fields of convective heat and/or mass transfer is still increasing. When the heat function and/or the mass function are made dimensionless in an adequate way, their values are closely related with the Nusselt and/or Sherwood numbers. The basics of the method were established in the 1980(s), and some novelties were subsequently added in order to increase the applicability range and facility of use of such visualization tools. Main steps included their use in unsteady problems, their use in polar cylindrical and spherical coordinate systems, development of similarity expressions for the heat function in laminar convective boundary layers, application of the method to turbulent flow problems, unification of the streamline, heatline, and massline methods (involving isotropic or anisotropic media), and the extension and unification of the method to apply to reacting flows. The method is now well established, and the efforts made towards unification resulted in very useful tools for visualization and analysis, which can be easily included in software packages for numerical heat transfer and fluid flow. This review describes the origins and evolution of the heatlines and masslines as visualization and analysis tools, from their first steps to the present. [DOI: 10.1115/1.2177684]

1 Introduction

When dealing with fluid flow, streamlines are well established as the most adequate and very useful tools to visualize two-dimensional incompressible flows from a long time ago (cf. [1]), and they are present in virtually any study or textbook on fluid dynamics. In a way similar to the streamlines, the heat flux lines are well established to visualize two-dimensional conductive heat transfer in isotropic media [2]. In this case, the heat flux lines are normal to the isotherms, and each one can be easily obtained from the other, and both are routinely used when dealing with conductive heat transfer.

When dealing with convective heat transfer, the isotherms are not the most adequate tools for visualization and analysis, and the heat flux lines are not necessarily perpendicular to them. Taken into consideration the total energy flux (enthalpy advection and heat diffusion), the heat flux lines, referred to as the heatlines, can also apply. The heat function and heatline concepts and formulation were originally introduced by Kimura and Bejan [3] in the 1980(s), and they appeared for the first time in a book on convective heat transfer by Bejan in 1984 [4]. Before that, convective heat transfer processes were analyzed using mainly the isotherms. But, the adequate visualizing tools in fluid dynamics are the streamlines and not the isobars, the same occurring in the field of convective heat transfer, where the adequate visualizing tools are the heatlines and not the isotherms.

A natural extension of the method was made to the field of convective mass transfer, through the introduction of the mass function and massline concepts by Trevisan and Bejan [5] in 1987.

If the heat function and/or the mass function are made dimensionless in an adequate way, their numerical values are closely related to the overall Nusselt and/or Sherwood numbers. In this way, they are very useful tools not only for visualization purposes but also for the analysis of the overall heat and/or mass transfer processes.

Once established the heatlines and masslines have been used as visualization and analysis tools of many and varied convective heat and mass transfer problems [3,5–13]. Some studies using the heatlines include thermomagnetic convection in electroconductive melts [14,15]. The heatline concept was also used for visualization and analysis of unsteady convective heat transfer, assuming that, at a given instant of analysis, the steady state version of the energy conservation equation is satisfied, as set forth by Aggarwal and Manhapra [16,17].

Application of the method to polar cylindrical coordinate systems was made firstly by Littlefield and Desai [18] to study the natural convection in a vertical cylindrical annulus, and later applied to some convection problems in circular annuli [19–21]. In the referred studies, the visualization using the heatlines is made in the r-θ plane [19,20], or in the r-z plane [18,21]. The method was also applied to polar spherical coordinate systems by Chattopadhyay and Dash [22], using the r-θ plane for visualization of the heatlines, where θ is the azimuthal angle.

The heatlines were also applied to some forced convection boundary layers, both in open [23] or fluid-saturated porous media [24], by developing the similarity expressions for the heatfunction corresponding to different heating or cooling wall conditions. Similarity expressions for the heat function were also obtained for laminar natural convection boundary layers adjacent to a vertical wall, considering different heating or cooling wall conditions [25].

The heatline concept was also applied when dealing with heat transfer in turbulent flows through the consideration of the turbulent fluxes into the heat function differential equation [26]. If the heat transfer problem under analysis occurs in the turbulent boundary layer near a wall, the heatline concept can be applied in a simpler way, by using an effective diffusion coefficient for heat, which includes the eddy diffusivity effect of the turbulent transport [27].

The heatline and massline methods evolved in a natural way,

Transmitted by Assoc. Editor E. Dowell.

and they appeared in a mature form in convection books, both in open fluid domains [27,28] and in porous domains [29]. In the recent book on convection heat transfer by Bejan [28], the method is used extensively. Once the method was established, some novelties were introduced in order to enlarge its applicability range and to ease its inclusion into computational fluid dynamics (CFD) codes and packages. The unification of the streamline, heatline, and massline methods, which are treated in a common way, was made by Costa [30], thus resulting in a general tool that can be easily included in CFD software codes and packages. This includes, for the first time, the possibility of variable diffusion coefficient for the function used for visualization purposes. Some controversy was associated with the treatment of such diffusion coefficients [10], but the adequate treatment is now well established [31]. The unified version of the streamline, heatline, and massline methods to apply to convective heat and mass transfer in anisotropic fluid-saturated porous media was also derived by Costa [32], which is of crucial importance when dealing with many natural or manufactured products, and it is a valuable tool that can be easily included in CFD codes and packages.

The last remarkable improvement of the method was made in order to apply it to reacting flows. As the method applies to divergence-free problems, special care should be taken when selecting the conserved variables to consider, without source terms in the governing differential equations. This was done by Mukhopadhyay et al. [33,34], by selecting as variables the normalized elemental mass fractions and the total enthalpy (formation enthalpy plus sensible enthalpy), with very encouraging results.

In what follows, presentation is made of the author's vision on the most important issues related with the development and application of the heatline and massline methods, and some illustrative examples of their application are also presented. A visit is made to the references involving the heatlines and masslines, both in what concerns new developments of the method or just its application. This is a work started before by Costa [35], but that, fortunately, needs to always be updated.

2 Origins of the Heat Function and Heatlines

2.1 Stream Function and Streamlines. The stream function and the streamlines are very useful tools when dealing with 2D fluid flow visualization and analysis, or even when dealing with 2D fluid flow calculations using a vorticity-stream function formulation.

For such situations, the mass conservation equation for an incompressible fluid reads

$$\frac{\partial}{\partial x}(\rho u)+\frac{\partial}{\partial y}(\rho v)=0 \tag{1}$$

Noting that ρu and ρv are the mass fluxes in the x and y directions, respectively, the stream function $\psi(x,y)$ can be introduced and defined through its first-order derivatives as

$$\frac{\partial \psi}{\partial y}=J_{m,x}=\rho u \tag{2a}$$

$$-\frac{\partial \psi}{\partial x}=J_{m,y}=\rho v \tag{2b}$$

Equation (1) is identically obtained evaluating and invoking the equality of the second-order crossed derivatives of $\psi(x,y)$.

The differential of the stream function $\psi(x,y)$ can be expressed as

$$d\psi=\frac{\partial \psi}{\partial x}dx+\frac{\partial \psi}{\partial y}dy=-J_{m,y}dx+J_{m,x}dy \tag{3}$$

or

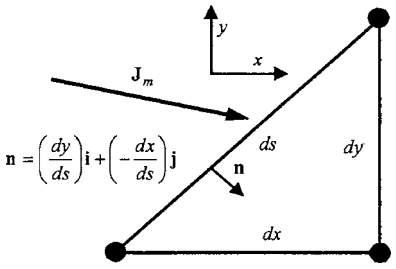

Fig. 1 Elementary segment $ds=\sqrt{dx^2+dy^2}$ crossed by the mass flux $\mathbf{J}_m$

$$d\psi=\mathbf{J}_m\cdot\mathbf{n}dA \tag{4}$$

where $\mathbf{n}$ is the outward normal of segment ds crossed by the flux $\mathbf{J}_m$, and $dA=ds\times 1$, as shown in Fig. 1 for a 2D system with a unit depth. If there is no mass flow crossing segment ds it is $d\psi=0$, and a line of constant ψ, a contour plot of ψ, is thus a line that is not crossed by mass. Mass flows between such ψ constant lines and, over such lines, it flows only tangentially to them. The ψ constant lines, the streamlines, thus define well bordered corridors, of impermeable walls, where mass flow occurs, which are very useful tools for flow visualization and analysis. As given by Eq. (4), the difference between the values of ψ corresponding to two lines of constant ψ is the mass flow rate that, by unit depth, flows between such lines.

Assuming that $\psi(x,y)$ is continuous to its second-order derivatives, Eq. (2*a*) can be differentiated with respect to y and Eq. (2*b*) can be differentiated with respect to x, and the results added to give

$$0=\frac{\partial^2 \psi}{\partial x^2}+\frac{\partial^2 \psi}{\partial y^2}+\left[\frac{\partial}{\partial x}(\rho v)-\frac{\partial}{\partial y}(\rho u)\right] \tag{5}$$

This is the second-order partial differential equation (a Poisson equation), from which the stream function field is obtained. Equation (5) can be solved once the flow field is known, evaluated using any available technique, a situation for which the source term of Eq. (5) (the symmetric of one-half of the vorticity) is already known, and, in this case, the stream function field is used to obtain the streamlines, the useful tools for 2D flow visualization and analysis. This same equation can, however, be solved as part of a vorticity-stream function formulation [36], and the stream function field is a primary field from which the velocity field can be obtained. In this case, from the stream function field it can also be directly obtained the streamlines used for flow visualization and analysis.

The streamlines have been used as visualization and analysis tools for a long time, and they are present in virtually every 2D flow study.

2.2 Heat Flux Lines for Heat Conduction Visualization. The analog of the stream function was also developed to apply to pure conduction heat transfer [2]. The steady energy conservation equation for a 2D situation without source term, and where only heat conduction in an isotropic medium of constant thermal conductivity is present, reads

$$0=\frac{\partial}{\partial x}\left(k\frac{\partial T}{\partial x}\right)+\frac{\partial}{\partial y}\left(k\frac{\partial T}{\partial y}\right) \tag{6}$$

Identifying the energy fluxes as $-k(\partial T/\partial x)$ and $-k(\partial T/\partial y)$, in the x and y directions, respectively, the stream function for heat transfer, $\psi_Q(x,y)$, can be defined through its first-order derivatives as

$$\frac{\partial \psi_Q}{\partial y}=J_{e,x}=-k\frac{\partial T}{\partial x} \tag{7a}$$

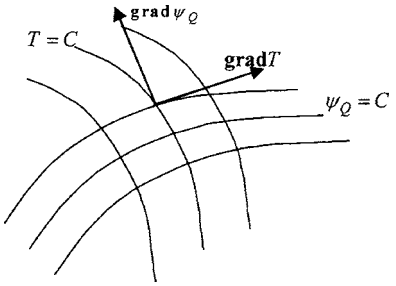

Fig. 2 Perpendicularity between the isotherms and the heat flux lines in heat conduction

$$-\frac{\partial \psi_Q}{\partial x} = J_{e,y} = -k\frac{\partial T}{\partial y} \tag{7b}$$

Equation (6) is identically obtained by adding the second-order mixed derivatives of $\psi_Q(x,y)$.

Assuming that $\psi_Q(x,y)$ is continuous to its second-order derivatives, Eq. (7*a*) can be differentiated with respect to y and Eq. (7*b*) can be differentiated with respect to x, and the obtained results added to give

$$0 = \frac{\partial^2 \psi_Q}{\partial x^2} + \frac{\partial^2 \psi_Q}{\partial y^2} \tag{8}$$

From this Laplace equation one obtains the $\psi_Q(x,y)$ field and, from it, the heat flux lines for visualization and analysis. Heat flows in such a way that the constant $\psi_Q(x,y)$ lines, the contour plots of $\psi_Q(x,y)$, are not crossed by heat.

For an isotropic medium of constant thermal conductivity, taking Eqs. (7*a*) and (7*b*), it is

$$\mathbf{grad}\, T \cdot \mathbf{grad}\, \psi_Q = 0 \tag{9}$$

that is, the heat flux lines are perpendicular to the isotherms, as illustrated in Fig. 2. Temperature acts like the potential for heat transfer, and heat flows as the current imposed by that potential.

In this way, the visualization and analysis of conduction heat transfer can be made using the isotherms, as the heat flux lines can be easily obtained or visualized as being perpendicular to the isotherms. However, when the medium is anisotropic or of variable thermal conductivity, or convection is present, the heat flux lines are not perpendicular to the isotherms, and new heat flux lines, the heatlines, need to be obtained following another way.

2.3 Heat Function and Heatlines. The heatlines were first proposed by Kimura and Bejan [3] in 1983, as the adequate tools for visualization and analysis of 2D convection heat transfer, through an extension of the heat flux line concept to include the advection terms.

The steady energy conservation equation for a 2D problem, without source term, reads

$$\frac{\partial}{\partial x}\left[\rho u c_p (T - T_0) - k\frac{\partial T}{\partial x}\right] + \frac{\partial}{\partial y}\left[\rho v c_p (T - T_0) - k\frac{\partial T}{\partial y}\right] = 0 \tag{10}$$

where T_0 is the reference temperature used for enthalpy referencing, and the constant pressure specific heat is used for gases or replaced by the specific heat, c, for incompressible liquids. In Eq. (10) are identified the energy flux components

$$J_{e,x} = \rho u c_p (T - T_0) - k\frac{\partial T}{\partial x} \tag{11a}$$

$$J_{e,y} = \rho v c_p (T - T_0) - k\frac{\partial T}{\partial y} \tag{11b}$$

and the heat function, $H(x,y)$, can be defined through its first-order derivatives as

$$\frac{\partial H}{\partial y} = J_{e,x} = \rho u c_p (T - T_0) - k\frac{\partial T}{\partial x} \tag{12a}$$

$$-\frac{\partial H}{\partial x} = J_{e,y} = \rho v c_p (T - T_0) - k\frac{\partial T}{\partial y} \tag{12b}$$

Equation (10) is obtained identically by adding the second-order crossed derivatives of $H(x,y)$ obtained from Eqs. (12*a*) and (12*b*), assuming that it is a continuous function to its second-order derivatives.

Similarly to what was explained for the streamlines and for the heat flux lines, a line of constant H, a contour plot of H, is a line that is not crossed by energy that is being transferred due to the combined effects of conduction and convection. The region between two lines of constant H behaves as a well bordered channel for energy transfer, or as a thermal energy tube. The difference between the values of H corresponding to two lines of constant H is the total energy flow rate that, by unit depth, flows between such lines. In this case, the isotherms and the heatlines are not perpendicular, and isotherms alone are only a poor tool for heat transfer visualization and analysis. When dealing with 2D fluid flow, it is not the isobars but the streamlines that are the best tools for visualization and analysis, as fluid flows not in the direction perpendicular to the isobars.

Similarly, when dealing with 2D convection heat transfer, it is not the isotherms but the heatlines that are the best tools for visualization and analysis, as energy does not flow in the direction perpendicular to the isotherms. Isotherms are still important as identifying the temperature levels in the domain, but they are poor and inadequate for heat transfer visualization and analysis.

From Eqs. (12*a*) and (12*b*) one obtains the second-order derivatives of the heat function, which can be added for a medium of constant thermal conductivity, to give the second-order differential equation (a Poisson equation) whose solution gives the heat function field

$$0 = \frac{\partial^2 H}{\partial x^2} + \frac{\partial^2 H}{\partial y^2} + \left\{\frac{\partial}{\partial x}[\rho v c_p (T - T_0)] - \frac{\partial}{\partial y}[\rho u c_p (T - T_0)]\right\} \tag{13}$$

The boundary conditions for this equation are obtained from the integration of the expressions for the H derivatives as given by the definition equations, Eqs. (12*a*) and (12*b*). For example, for a rectangular domain, over a vertical boundary the values of H are specified, using Eq. (12*a*), as

$$H(x_B, y) = H(x_B, y_{\text{ref}}) + \int_{y_{\text{ref}}}^{y} \left[\rho u c_p (T - T_0) - k\frac{\partial T}{\partial x}\right]_{x_B} dy \tag{14}$$

y_{ref} being a point where the H value is known by any way. It should be noted that, given the way in which the heat function is defined, through its first-order derivatives, only the differences in the H values are important and not the H level itself. If the vertical boundary under analysis is such that the velocity is zero there, Eq. (14) simplifies to give

$$H(x_B, y) = H(x_B, y_{\text{ref}}) + \int_{y_{\text{ref}}}^{y} \left(-k\frac{\partial T}{\partial x}\right)_{x_B} dy \tag{15}$$

The reference temperature, T_0, used in the H definition equations, Eqs. (12*a*) and (12*b*), arises from the fact that the energy fluxes include two distinct components: Fourier conduction and enthalpy flow. As the enthalpy property needs to be referenced to

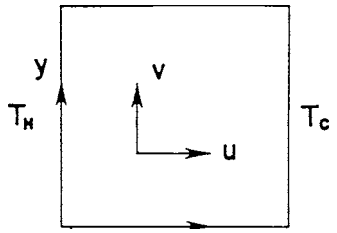

Fig. 3 Physical model and geometry for the work of Kimura and Bejan [3] (reprinted with permission from [3])

a given state, this is chosen as the one corresponding to temperature T_0. Selection of T_0 is arbitrary, but it has an influence on the obtained heatlines, given that different values of T_0 lead to different slopes of the H field, as given by Eqs. (12*a*) and (12*b*). The value of T_0 is irrelevant in what concerns the energy conservation equation; once invoked the mass conservation equation, the terms involving T_0 vanish in the energy conservation equation. This is different, however, in the differential equation governing the H field, Eq. (13), whose source term depends on T_0. In order to solve this problem, a unified treatment has been proposed by Bejan [27], by setting T_0 as the minimum temperature level in the domain under analysis.

The first heatline patterns were published by Kimura and Bejan [3] for the natural convection problem in a differentially heated square enclosure presented in Fig. 3, whose top and bottom boundaries are perfectly insulated. Some of such results, in the form of heatlines are presented in Fig. 4(*a*) for $\mathrm{Ra}_Y=140$ and in Fig. 4(*b*) for $\mathrm{Ra}_Y=1.4\times10^5$, where $\mathrm{Ra}_Y=g\beta(T_H-T_C)Y^3/(\nu\alpha)$ is the Y-based Rayleigh number.

In Fig. 4(*a*), for a low Rayleigh number, flow intensity is very low, and heat transfer occurs mainly by conduction. Isotherms are nearly vertical, and the heatlines are nearly horizontal, as expected for a conduction dominated problem. It is also observed that heat leaves the hot wall in an almost uniform way, and reaches the cold wall also in an almost uniform way. However, for a high Rayleigh number, as presented in Fig. 4(*b*), the flow intensity is observed and the isotherms are far from the vertical form. It is observed that heat transfer is more intense at the lower-left and upper-right regions of the enclosure's vertical walls, and that their upper-left and lower-right regions only have a poor contribution for heat transfer. This is typical for this problem, as shown by the local Nusselt number results presented by Costa [9]. In this case, the heatlines are the adequate tools for visualization and analysis of the heat transfer process, giving well defined corridors where energy transfer occurs from the hot wall towards the cold wall. Near the vertical walls, where velocity is low and conduction is dominant, the heatlines have a markedly horizontal profile. When dealing with heat transfer visualization and analysis, the heatlines show thus to be the effective tools to do that, and the picture given by the isotherms is only of minor relevance for that.

For a problem like the natural convection in a differentially heated square enclosure, the overall Nusselt number is usually defined as

$$\mathrm{Nu}=\frac{\dot{Q}_{\mathrm{convection}}}{\dot{Q}_{\mathrm{conduction}}}=\frac{\displaystyle\int_0^Y\left(-k\frac{\partial T}{\partial x}\right)_{x=0}dy}{kY(T_H-T_C)/Y} \tag{16}$$

Making the heat function dimensionless as $H_*=H/[k(T_H-T_C)]$, and taking into account Eq. (15), Eq. (16) can be expressed as

$$\mathrm{Nu}=H_*(x_B,Y)-H_*(x_B,y_{\mathrm{ref}}) \tag{17}$$

If $y_{\mathrm{ref}}=0$ and it is set that $H_*(x_B,y_{\mathrm{ref}})=0$, the overall Nusselt number becomes equal to the maximum value of the heat function, an important result when visualizing and analyzing heat transfer processes using the heat function and heatlines. It should be referred that for a situation where pure conduction heat transfer is present and fluid flow subsides, the heat function coincides with the stream function for heat flow, $\psi_Q(x,y)$, as explained in Sec. 2.2.

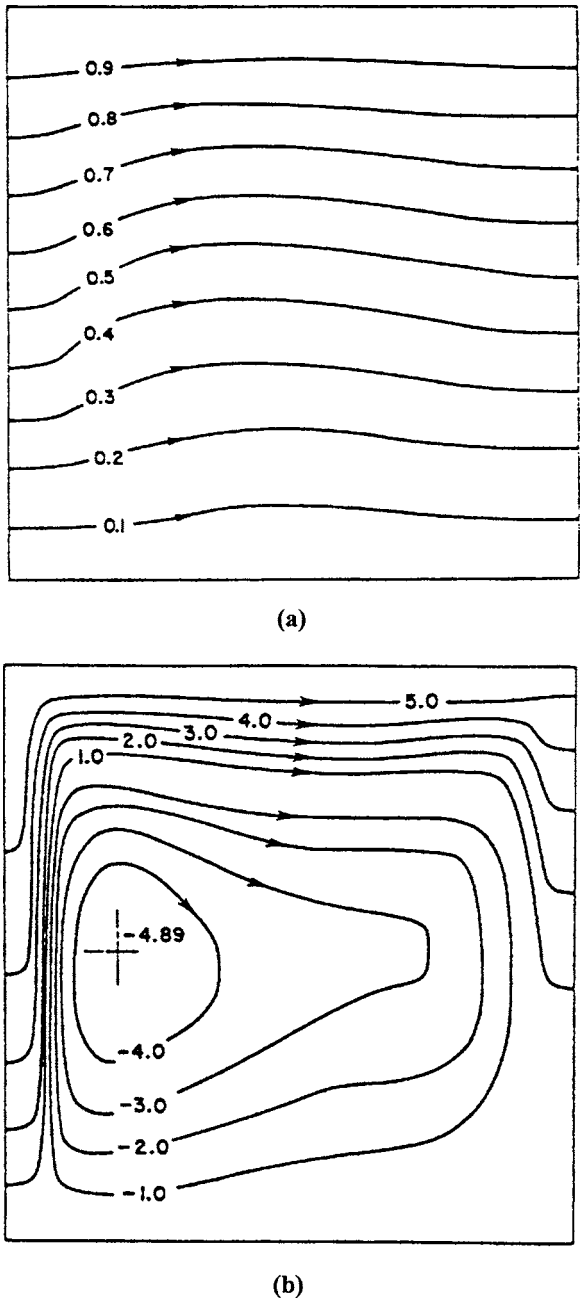

Fig. 4 Heatlines in the work of Kimura and Bejan [3], for Pr =7 and (*a*) Ra=140 and (*b*) Ra=1.4×10^5 (reprinted with permission from [3])

3 Mass Function and Masslines

The concept of heat function and heatlines was extended to the field of convective mass transfer by Trevisan and Bejan [5] in 1987, thus coining the terms of mass function and masslines.

The 2D steady mass conservation equation for a given particular chemical species i, without source term, reads

$$\frac{\partial}{\partial x}\left[\rho u(C_i - C_{i,0}) - \rho D_i \frac{\partial C_i}{\partial x}\right] + \frac{\partial}{\partial y}\left[\rho v(C_i - C_{i,0}) - \rho D_i \frac{\partial C_i}{\partial y}\right] = 0 \tag{18}$$

where $C_{i,0}$ is the minimum value of the mass concentration of component i, similarly to what was made for the reference temperature T_0 in Eq. (10). Identifying the mass flux components of species i as

$$J_{m_i,x} = \rho u(C_i - C_{i,0}) - \rho D_i \frac{\partial C_i}{\partial x} \tag{19a}$$

$$J_{m_i,y} = \rho v(C_i - C_{i,0}) - \rho D_i \frac{\partial C_i}{\partial y} \tag{19b}$$

the mass function for this particular chemical species, $M_i(x,y)$, can be defined through its first-order derivatives as

$$\frac{\partial M_i}{\partial y} = J_{m_i,x} = \rho u(C_i - C_{i,0}) - \rho D_i \frac{\partial C_i}{\partial x} \tag{20a}$$

$$-\frac{\partial M_i}{\partial x} = J_{m_i,y} = \rho v(C_i - C_{i,0}) - \rho D_i \frac{\partial C_i}{\partial y} \tag{20b}$$

The second-order derivatives of $M_i(x,y)$ can be obtained from Eqs. (20*a*) and (20*b*), and the results added, for a medium with constant ρD_i, to give the second-order partial differential equation (a Poisson equation) from which the mass function field is evaluated

$$0 = \frac{\partial^2 M_i}{\partial x^2} + \frac{\partial^2 M_i}{\partial y^2} + \left\{\frac{\partial}{\partial x}[\rho v(C_i - C_{i,0})] - \frac{\partial}{\partial y}[\rho u(C_i - C_{i,0})]\right\}. \tag{21}$$

This equation is formally similar to Eq. (13), obtained for the heat function. The boundary conditions for the mass function are set in a way similar to that explained for the heat function.

The first results involving the mass function and the masslines were presented by Trevisan and Bejan [5] for the double-diffusive natural convection problem in a square enclosure subjected to constant wall heat and mass fluxes. Some of these results are presented in Fig. 5. As referred to in the paper of Trevisan and Bejan [5], the particular reference value $C_{i,0}$ was taken as the enclosure-averaged quantity (measured at the center of the enclosure), in search of centrosymmetric massline patterns. In this case, as the wall mass flux is constant, the masslines are equally spaced at the left and right vertical walls of the enclosure. Once again, and similarly to what happened with the heatlines for heat transfer visualization, it is observed that the masslines define well bordered corridors where mass flows, and that they are the effective tools for mass transfer visualization and analysis, and not the isoconcentration lines.

Also in this case, the mass function can be made dimensionless in such a way that its maximum value equals the overall Sherwood number relative to the particular chemical species under analysis.

As a limiting situation, consider the case when the fluid is a single component medium, for which there is no mass diffusion, the mass conservation equation reduces to the global mass conservation equation, Eq. (1), the mass function is the same as the stream function, and the masslines are the same as the streamlines.

4 Heat Function and Heatlines in Polar Coordinate Systems

4.1 Cylindrical Coordinate Systems. The mass conservation equation in the cylindrical coordinate system, when the phenomena under interest occur in the r-θ plane, reads [37]

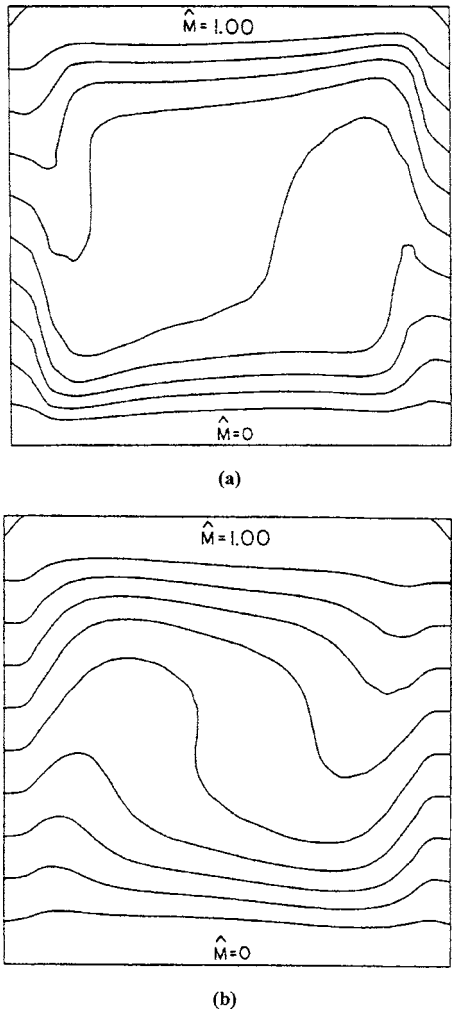

Fig. 5 Masslines for the double-diffusive natural convection problem in a square enclosure subjected to constant wall heat and mass fluxes for Ra=3.5×10⁵, Le=1, Pr=7 and (*a*) *N*=−4 and (*b*) *N*=−0.9 (reprinted with permission from [5])

$$\frac{1}{r}\frac{\partial}{\partial r}(\rho r v_r) + \frac{1}{r}\frac{\partial}{\partial \theta}(\rho v_\theta) = 0 \tag{22}$$

and the corresponding energy conservation equation reads

$$\frac{1}{r}\frac{\partial}{\partial r}[\rho r v_r c_p(T - T_0)] + \frac{1}{r}\frac{\partial}{\partial \theta}[\rho v_\theta c_p(T - T_0)] = \frac{1}{r}\frac{\partial}{\partial r}\left(kr\frac{\partial T}{\partial r}\right) + \frac{1}{r}\frac{\partial}{\partial \theta}\left(\frac{k}{r}\frac{\partial T}{\partial \theta}\right) \tag{23}$$

This last equation can be rewritten as

$$\frac{1}{r}\frac{\partial}{\partial r}\left[\rho r v_r c_p(T - T_0) - kr\frac{\partial T}{\partial r}\right] + \frac{1}{r}\frac{\partial}{\partial \theta}\left[\rho v_\theta c_p(T - T_0) - \frac{k}{r}\frac{\partial T}{\partial \theta}\right] = 0 \tag{24}$$

From Eq. (24) it can be identified the energy fluxes in the r and θ directions, and the heat function $H(r,\theta)$ can be defined through its first-order derivatives as

$$\frac{\partial H}{\partial \theta} = \rho r v_r c_p(T - T_0) - kr\frac{\partial T}{\partial r} \tag{25a}$$

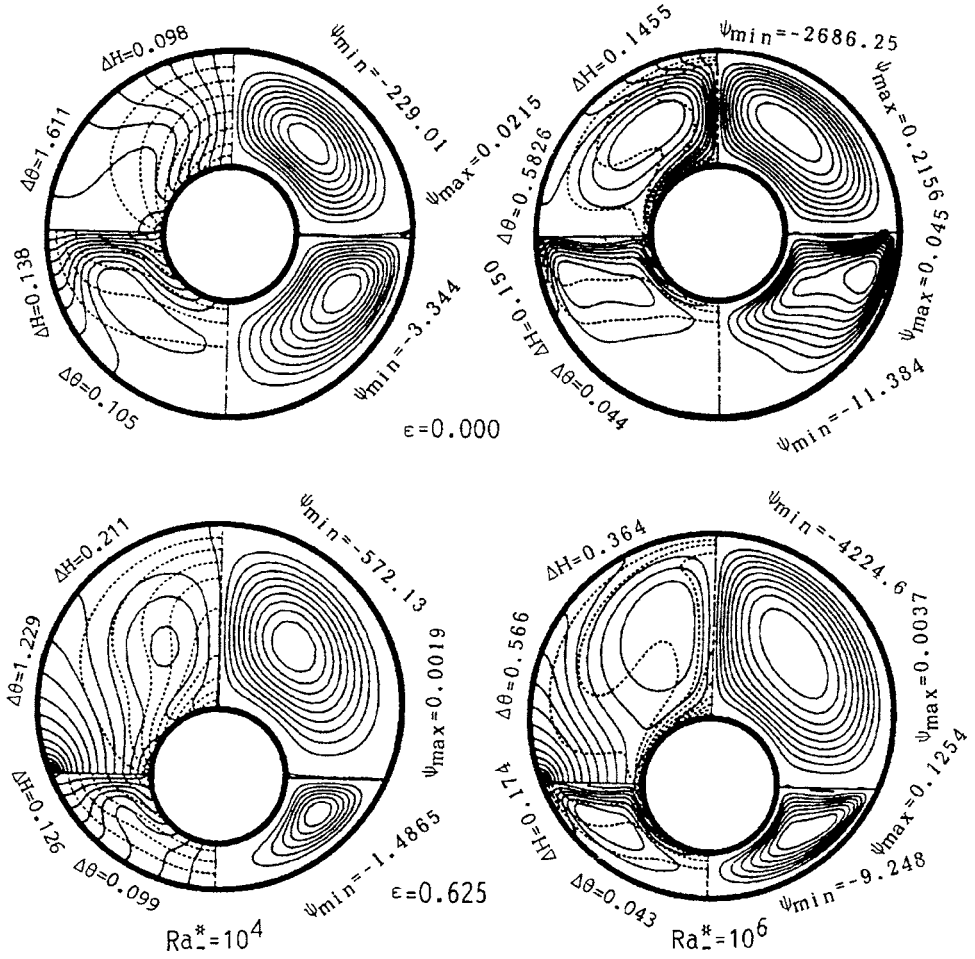

Fig. 6 Streamlines (right) and heatlines (left) (isotherms are the dashed lines) for the thermogravitational convection in concentric and eccentric annuli, for different values of the Rayleigh number (reprinted with permission from [19])

$$-\frac{\partial H}{\partial r}=\rho v_\theta c_p(T-T_0)-\frac{k}{r}\frac{\partial T}{\partial \theta} \tag{25b}$$

Evaluating the second-order crossed derivatives of $H(r,\theta)$ from Eqs. (25*a*) and (25*b*), Eq. (24) is identically obtained.

If, instead, the plane of interest is the r-z plane, the mass conservation equation reads [37]

$$\frac{1}{r}\frac{\partial}{\partial r}(\rho r v_r)+\frac{\partial}{\partial z}(\rho v_z)=0 \tag{26}$$

and the corresponding energy conservation equation reads

$$\frac{1}{r}\frac{\partial}{\partial r}[\rho r v_r c_p(T-T_0)]+\frac{\partial}{\partial z}[\rho v_z c_p(T-T_0)]$$
$$=\frac{1}{r}\frac{\partial}{\partial r}\left(kr\frac{\partial T}{\partial r}\right)+\frac{\partial}{\partial z}\left(k\frac{\partial T}{\partial z}\right) \tag{27}$$

which can be rewritten as

$$\frac{1}{r}\frac{\partial}{\partial r}\left[\rho r v_r c_p(T-T_0)-kr\frac{\partial T}{\partial r}\right]+\frac{\partial}{\partial z}\left[\rho v_z c_p(T-T_0)-k\frac{\partial T}{\partial z}\right]=0 \tag{28}$$

From this last equation it can be identified the energy fluxes in the r and z directions, and the heat function $H(r,z)$ can be defined through its first-order derivatives as

$$\frac{\partial H}{\partial z}=\rho r v_r c_p(T-T_0)-kr\frac{\partial T}{\partial r} \tag{29a}$$

$$-\frac{1}{r}\frac{\partial H}{\partial r}=\rho v_z c_p(T-T_0)-k\frac{\partial T}{\partial z} \tag{29b}$$

Evaluating the second-order crossed derivatives of $H(r,z)$ from Eqs. (29*a*) and (29*b*), Eq. (28) is identically obtained.

The second-order differential equation, from which the $H(r,\theta)$ or the $H(r,z)$ field is evaluated, is obtained adding the second-order derivatives of H obtained from the first-order derivatives defining it, similarly to what was made for the Cartesian coordinate system.

Results, in the form of streamlines and heatlines in the r-θ plane, were obtained by Ho and Lin [19,20] for air/water layers enclosed in horizontal annuli, some of which are presented in Fig. 6.

Results, in the form of streamlines and heatlines in the r-z plane, were obtained by Littlefield and Desai [18] and by Ho and Lin [21] for a vertical cylindrical annulus.

4.2 Spherical Coordinate Systems. When the system under analysis is better described using the spherical coordinate system, in the r-θ plane, where θ is the azimuthal direction, the mass conservation equation reads [37]

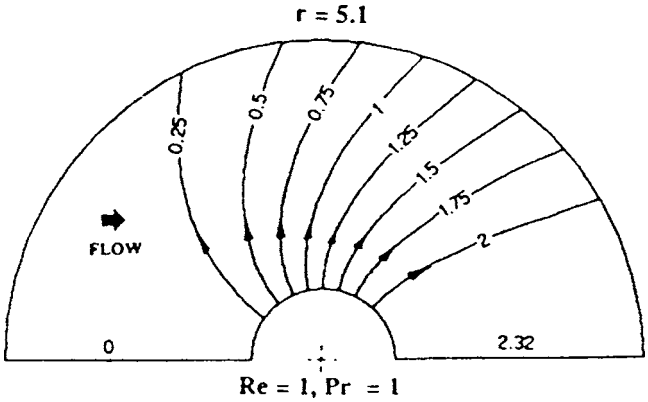

Fig. 7 Heatlines in a solid sphere subjected to cooling (reprinted with permission from [22])

$$\frac{1}{r^2}\frac{\partial}{\partial r}(\rho r^2 v_r) + \frac{1}{r\sin\theta}\frac{\partial}{\partial\theta}(\rho v_\theta \sin\theta) = 0 \tag{30}$$

and the energy conservation equation reads

$$\frac{1}{r^2}\frac{\partial}{\partial r}[\rho r^2 v_r c_p(T-T_0)] + \frac{1}{r\sin\theta}\frac{\partial}{\partial\theta}[\rho v_\theta \sin\theta c_p(T-T_0)] = \frac{1}{r^2}\frac{\partial}{\partial r}\left(r^2 k\frac{\partial T}{\partial r}\right) + \frac{1}{r\sin\theta}\frac{\partial}{\partial\theta}\left(\frac{k}{r}\sin\theta\frac{\partial T}{\partial\theta}\right) \tag{31}$$

which can be rewritten as

$$\frac{1}{r^2}\frac{\partial}{\partial r}\left[\rho r^2 v_r c_p(T-T_0) - r^2 k\frac{\partial T}{\partial r}\right] + \frac{1}{r\sin\theta}\frac{\partial}{\partial\theta}\left[\rho v_\theta \sin\theta c_p(T-T_0) - \frac{k}{r}\sin\theta\frac{\partial T}{\partial\theta}\right] = 0 \tag{32}$$

From this last equation it can be identified the energy fluxes in the r and θ directions, and the heat function $H(r,\theta)$ in the spherical coordinate system can be defined through its first-order derivatives as

$$\frac{1}{\sin\theta}\frac{\partial H}{\partial\theta} = \rho r^2 v_r c_p(T-T_0) - r^2 k\frac{\partial T}{\partial r} \tag{33a}$$

$$-\frac{1}{r}\frac{\partial H}{\partial r} = \rho v_\theta \sin\theta c_p(T-T_0) - \frac{k}{r}\sin\theta\frac{\partial T}{\partial\theta} \tag{33b}$$

Evaluating the second-order crossed derivatives of $H(r,\theta)$ from Eqs. (33*a*) and (33*b*), Eq. (32) is identically obtained.

The second-order differential equation, from which the $H(r,\theta)$ field is evaluated, is obtained adding the second-order derivatives of H obtained from the first-order derivatives defining it, similarly to what was made before for the Cartesian coordinate system.

Results, in the form of heatlines, were obtained by Chattopadhyay and Dash [22] for the study of convective heat transfer from a sphere. Some of these results are presented in Fig. 7.

The presented results, concerning the use of the heatlines for visualization and analysis of convective heat transfer occurring in systems that are naturally adapted to polar coordinate systems, also emphasize the usefulness of such visualization tools, which are the adequate tools for energy path identification and global quantification in convection heat transfer.

5 Heatlines and Masslines in Fluid-Saturated Porous Media

When dealing with fluid-saturated porous media, the steady global mass conservation equation is still Eq. (1), the steady energy conservation equation, without source term, is still Eq. (10), and the steady mass conservation equation for the particular chemical species i is still Eq. (18). In this case, the thermal conductivity results from the combination of the thermal conductivities of both fluid and porous matrix, and the effective mass diffusivity results from the combination of the diffusivities of both fluid and porous matrix. The velocity components are volume averaged values, usually referred to as Darcy velocity components [29], which are evaluated using any reasonable physical model [29], always under the condition that mass must be satisfied.

In this way, the streamlines, heatlines and masslines, as presented before, also apply for 2D steady heat and mass transfer convective problems in fluid-saturated porous media.

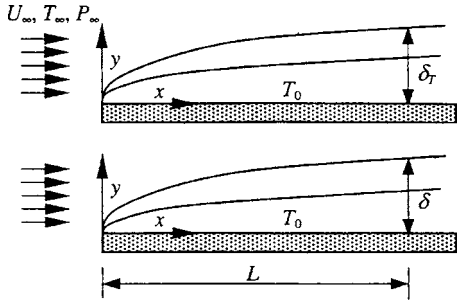

Fig. 8 Boundary layer in forced convection near a flat plate for a fluid with Pr<1 (top) and for a fluid with Pr>1 (bottom)

6 Use of Heatlines in Unsteady Problems

Strictly, heatlines and masslines can be used only for 2D divergence-free situations, that is, for 2D steady problems without source terms.

The energy conservation equation for an unsteady problem, without source term, reads

$$\frac{\partial}{\partial t}(\rho c_p T) + \frac{\partial}{\partial x}\left[\rho u c_p(T-T_0) - k\frac{\partial T}{\partial x}\right] + \frac{\partial}{\partial y}\left[\rho v c_p(T-T_0) - k\frac{\partial T}{\partial y}\right] = 0 \tag{34}$$

which is not a divergence-free equation. However, considering that, at a given instant, the differential energy conservation equation without the unsteady term can be taken to describe the heat transfer problem, the heatline concept can be applied without problems to such an equation. This has been made successfully by Aggarwal and Manhapra [16,17] to analyze the unsteady heat transfer process in cylindrical enclosures subjected to natural convection.

It should be refereed, however, that such a procedure is acceptable in problems with small unsteady terms when compared with the diffusive and/or convective terms, for which the steady energy conservation equation gives a good description at a given instant. Otherwise, if the unsteady term is not so small, the steady energy conservation equation is only a poor, or even unrealistic, description of the involved heat transfer process at a given instant. From the viewpoint of the energy conservation equation, the unsteady term can be interpreted also as a source (volumetric) term.

The considerations made about the use of the heatlines for unsteady problems apply equally to the use of masslines for unsteady problems.

7 Heat Function and Heatlines in Boundary Layer Problems–Similarity Solutions

7.1 Forced Convection. Once verified some conditions, the steady flow and energy problems near a flat plate, like that in Fig. 8, for a fluid of constant properties, can be described by the mass conservation equation, Eq. (1), by the momentum boundary layer

equation, and by the boundary layer energy conservation equation. These equations read, respectively, as given by Bejan [27]

$$\frac{\partial u}{\partial x}+\frac{\partial v}{\partial y}=0 \tag{35}$$

$$u\frac{\partial u}{\partial x}+v\frac{\partial u}{\partial y}=\nu\frac{\partial^2 u}{\partial y^2} \tag{36}$$

$$\rho c_P\left(u\frac{\partial T}{\partial x}+v\frac{\partial T}{\partial y}\right)=k\frac{\partial^2 T}{\partial y^2} \tag{37}$$

A similarity solution can be obtained for the flow problem, and also for the heat transfer problem. As the flow is forced, and it is not influenced by the temperature field, the similarity solution for the flow problem is obtained first. The developments that follow are essentially due to Al Morega and Bejan [23].

Making the Cartesian coordinates dimensionless as $x_*=x/L$ and $y_*=(y/L)\mathrm{Re}_L^{1/2}$, where $\mathrm{Re}_L=U_\infty L/\nu$ as is the L-based Reynolds number, it can be defined as the dimensionless similarity variable as

$$\eta(x_*,y_*)=(y/x)\mathrm{Re}_x^{1/2}=y_* x_*^{-1/2} \tag{38}$$

where $\mathrm{Re}_x=U_\infty x/\nu$ is the x-based Reynolds number. The stream function is made dimensionless as $\psi_*=\psi/(U_\infty L)$, and it can be expressed as

$$\psi_*(x_*,\eta)=\mathrm{Re}_L^{-1/2}\,x_*^{1/2} f(\eta) \tag{39}$$

where $f(\eta)$ is the dimensionless similarity function.

The dimensionless velocity components $(u_*,v_*)=(u,v)/U_\infty$ are obtained from the dimensionless stream function as

$$u_*=\mathrm{Re}_L^{1/2}(\partial\psi_*/\partial y_*)=f' \tag{40a}$$

$$v_*=-\partial\psi_*/\partial x_*=\tfrac{1}{2}\,\mathrm{Re}_L^{-1/2}\,x_*^{-1/2}(\eta f'-f) \tag{40b}$$

where $f'=df/d\eta$ and it should be noted that the reference lengths used to make the space coordinates dimensionless are related by $\mathrm{Re}_L^{1/2}$. Thus, once the solution of the similarity function is known, the stream function is known and the velocity components are also known.

Substitution of the dimensionless velocity components, as given by Eqs. (40*a*) and (40*b*), into the momentum boundary layer equation, Eq. (36), leads to

$$2f'''+ff''=0 \tag{41}$$

an ordinary differential equation subjected to the boundary conditions $f(0)=f'(0)=0$ and $f'(+\infty)=1$. Equation (41) depends only on the η variable, and the main advantage of the similarity transformation is the reduction of the number of independent variables from two, x,y, to one, η. The solution of the boundary layer flow problem is evaluated from the solution of Eq. (41).

Once the flow solution is known, the heat transfer problem can also be solved using the similarity transformation. Substitution of the velocity components as given by Eqs. (40*a*) and (40*b*) into the boundary layer energy conservation equation, Eq. (37), making the temperature dimensionless as $\theta(x,y)=[T(x,y)-T_w]/(T_\infty-T_w)$, one obtains

$$\theta''+(\mathrm{Pr}/2)f\theta'=0 \tag{42}$$

where it can be made $T(x,y)=T(\eta)$, and $\theta=\theta(\eta)$ only. The heat transfer problem is solved once the solution of Eq. (42) is known, subjected to the boundary conditions $\theta(0)=0$ and $\theta(+\infty)=1$.

The heat function for this problem is defined using the expressions given by Eqs. (12*a*) and (12*b*), noting that, in this case, the diffusive term in Eq. (12*a*) does not exist. The heat function is made dimensionless using the convective term and not the diffusive term as made before, through the expression

$$H_*=\frac{H}{\rho c_P U_\infty|T_\infty-T_w|L\,\mathrm{Re}_L^{-1/2}} \tag{43}$$

where $|T_\infty-T_w|=T_\infty-T_w$ for an isothermal cold wall and $|T_\infty-T_w|=T_w-T_\infty$ for an isothermal hot wall.

It should be noted that the global heat transfer between the wall of length L and the stream can be obtained, in a scale sense, from an energy balance made to the thermal boundary layer. Such energy balace gives $\dot{Q}\sim\dot{m}c_P(T_\infty-T_w)=\rho u c_P(T_\infty-T_w)\delta_T$, where δ_T is the thickness of the thermal boundary layer and u is the velocity at the leading edge of the thermal boundary layer. For a fluid with $\mathrm{Pr}<1$ it is $\delta_T\sim L\,\mathrm{Pr}^{-1/2}\,\mathrm{Re}_L^{-1/2}$ and $u\sim U_\infty$, and it is $\dot{Q}\sim\rho U_\infty c_P(T_\infty-T_w)L\,\mathrm{Re}_L^{-1/2}\,\mathrm{Pr}^{-1/2}$. For a fluid with $\mathrm{Pr}>1$ it is $\delta_T\sim L\,\mathrm{Pr}^{-1/3}\,\mathrm{Re}_L^{-1/2}$ and $u\sim U_\infty(\delta_T/\delta)$, and it is $\dot{Q}\sim\rho U_\infty c_P(T_\infty-T_w)L\,\mathrm{Re}_L^{-1/2}\,\mathrm{Pr}^{-2/3}$. In this way, as $\dot{Q}\sim hL(T_\infty-T_w)$ and $\mathrm{Nu}=hL/k$, it is $\mathrm{Nu}\sim\dot{Q}/[k(T_\infty-T_w)]$. The overall Nusselt number is proportional to $\mathrm{Re}^{1/2}\,\mathrm{Pr}^{1/2}$ for a fluid with $\mathrm{Pr}<1$, and the overall Nusselt number is proportional to $\mathrm{Re}^{1/2}\,\mathrm{Pr}^{1/3}$ for a fluid with $\mathrm{Pr}>1$. These proportionalities have been explored in depth by Al Morega and Bejan [23].

The dimensionless first-order derivatives that define the heat-function near an isothermal cold wall become

$$\frac{\partial H_*}{\partial y_*}=f'\theta \tag{44a}$$

$$-\frac{\partial H_*}{\partial x_*}=\frac{1}{2}x_*^{-1/2}(\eta f'-f)\theta-\frac{1}{\mathrm{Pr}}\frac{\partial\theta}{\partial y_*} \tag{44b}$$

and it is assumed that $H_*(x_*,y_*)$ is given by an expression of the form

$$H_*(x_*,y_*)=x_*^{1/2}g[\eta(x_*,y_*)] \tag{45}$$

Function g is found to be

$$g(\eta)=f\theta+\frac{2}{\mathrm{Pr}}\theta' \tag{46}$$

which gives, for the similarity solution for the heat function

$$H_*(x_*,\eta)=x_*^{1/2}\left(f\theta+\frac{2}{\mathrm{Pr}}\theta'\right) \tag{47}$$

under the assumption that $H_*(0,0)=0$.

Similarly it can be obtained the similarity solution for the heat function near an isothermal hot wall as

$$H_*(x_*,\eta)=-x_*^{1/2}\left[f(\theta-1)+\frac{2}{\mathrm{Pr}}\theta'\right] \tag{48}$$

also under the assumption that $H_*(0,0)=0$.

At the wall it is $\eta=0$ and $f(0)=0$, and θ' is a function of the Prandtl number only, as given by Bejan [27], and the heat function increases with $x_*^{1/2}$ along the cold wall and decreases with $-x_*^{1/2}$ along the hot wall.

Some of the results obtained by Al Morega and Bejan [23] are presented in Fig. 9(*a*) for an isothermal hot wall and in Fig. 9(*b*) for an isothermal cold wall.

Heatlines give a very good picture about how heat leaves the hot wall towards the free stream in Fig. 9(*a*), and how heat leaves the hot stream towards the cold wall in Fig. 9(*b*). It is also clear in these figures that the heat transfer process occurs in a region, the thermal boundary layer, which is thinner than the velocity boundary layer, as expected and explained by Bejan [27] for a fluid with $\mathrm{Pr}>1$. For a fluid with $\mathrm{Pr}=0.02$, the thermal boundary layer is thicker than the velocity boundary layer, as shown in Fig. 10(*a*) for a hot isothermal wall and in Fig 10(*b*) for a cold isothermal

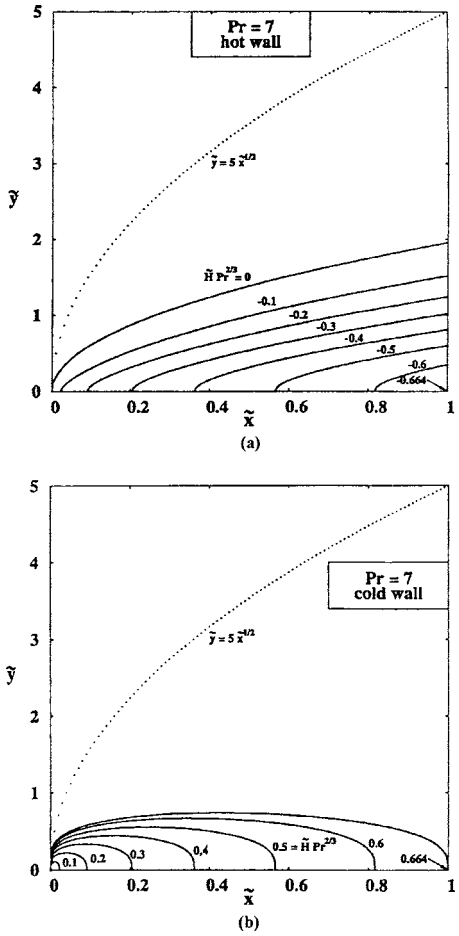

Fig. 9 Heatlines obtained from the similarity solution of the heatfunction for the forced convection near a flat plate, for Pr =7 (*a*) near a hot isothermal wall and (*b*) near a cold isothermal wall (reprinted with permission from [23])

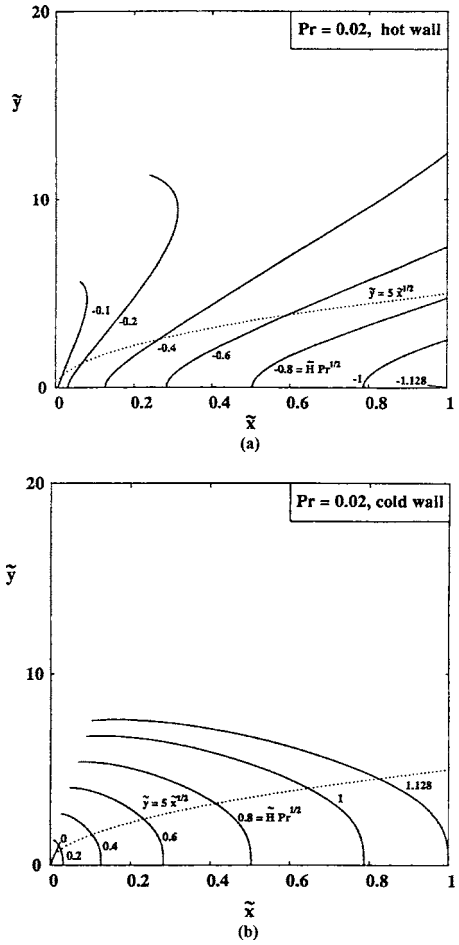

Fig. 10 Heatlines obtained from the similarity solution of the heat function for the forced convection near a flat plate, for Pr=0.02 (*a*) near a hot isothermal wall and (*b*) near a cold isothermal wall (reprinted with permission from [23]

wall.

The similarity solution for the heat function can also be obtained for the situation of a hot wall with uniform heat flux. In this case, the temperature in the boundary layer changes as

$$T(x,y) = T_\infty + \frac{\dot{q}''}{k}\left(\frac{\nu x}{U_\infty}\right)^{1/2}\theta(\eta) \tag{49}$$

and the similarity version of the heat transfer problem is given by the equation

$$\theta'' + \frac{\mathrm{Pr}}{2}(f\theta' - f'\theta) = 0 \tag{50}$$

satisfying the boundary conditions $\theta'(0)=-1$ and $\theta(+\infty)=0$.

In this case, the heat function is made dimensionless as

$$H_*(x_*,y_*) = \frac{H(x,y)}{\dot{q}''L} \tag{51}$$

noting that $\dot{q}''L$ is the global heat transfer exchange between the wall and the fluid, and the first-order derivatives that define the heat function are

$$\frac{\partial H_*}{\partial y_*} = \mathrm{Pr}\, x_*^{1/2} f'\theta \tag{52a}$$

$$-\frac{\partial H_*}{\partial x_*} = \tfrac{1}{2}\,\mathrm{Pr}(\eta f' - f)\theta - \theta' \tag{52b}$$

Following a similar procedure as for the isothermal wall, the similarity solution for the heat function becomes

$$H_*(x_*,\eta) = x_*\left(\frac{1}{2}\,\mathrm{Pr}\, f\theta + \theta'\right) \tag{53}$$

also with $H_*(0,0)=0$. In this case, as $f(0)=0$ and $\theta'(0)=-1$ it is $H_*(x_*,0)=-x_*$ and the heat function value at the wall decreases linearly with $-x_*$ along the wall length, as expected due to the constant heat flux there.

Similar studies were conducted by Al Morega and Bejan [24] for the forced convection boundary layer in porous media. This is the first reported study where heatlines were applied to fluid-saturated porous media. The development is similar but simpler, as the v velocity component was taken as zero in the thermal boundary layer inside the porous medium. In this study, Al Morega and Bejan [24] considered the situations of isothermal hot and cold wall, and the situation of uniform heat flux hot wall. The obtained results are similar in form to those corresponding to the open fluid domain, and equally rich in what concerns the picture given by the heatlines about the heat transfer process.

In this same work, Al Morega and Bejan [24] considered the internal convection in a confined porous medium inside a parallel plate channel. The fluid is assumed to flow uniformly inside the porous domain, with $u=U$ and $v=0$. Assuming fully developed

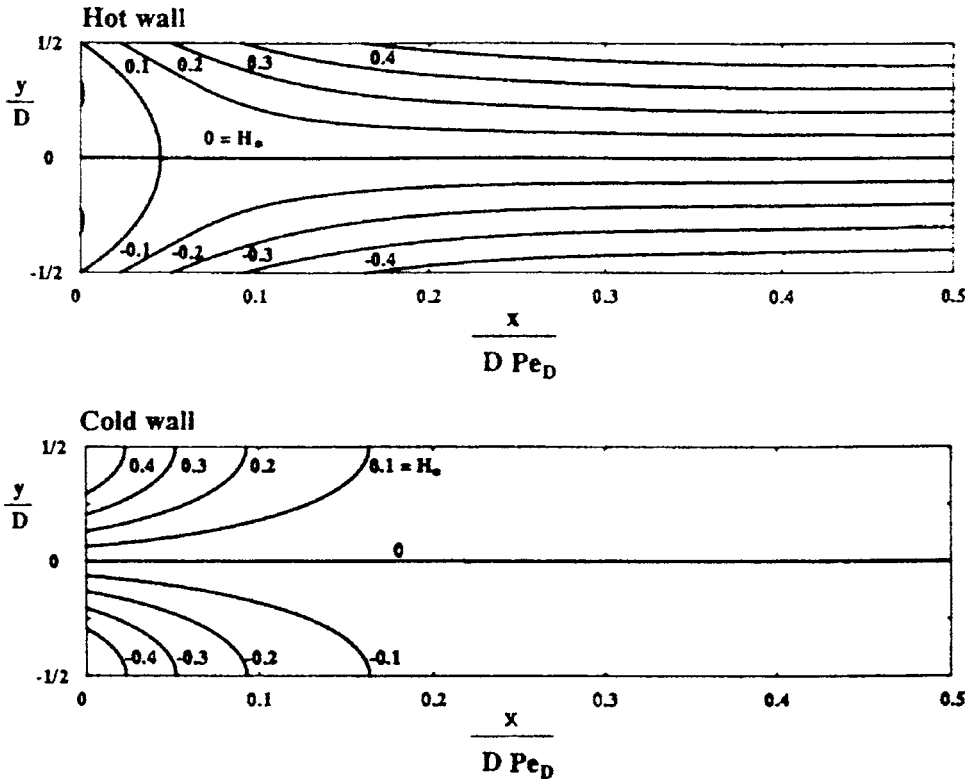

Fig. 11 Heatlines obtained from the analytical solution of the heat function for the forced convection in a fluid-saturated porous medium inside a channel. (Top) Near a hot isothermal wall and (bottom) near a cold isothermal wall (reprinted with permission from [24]).

conditions, closed analytical solutions were obtained for the heat function, for situations where the channel walls are isothermal and cold or hot. The obtained results are presented in Fig. 11, where a clear and rich picture is obtained about the heat transfer process taking place.

For comparison purposes, closed analytical expressions for the heat function were also obtained by Al Morega and Bejan [24] for the pure fluid in slug flow inside the channel, with $u=U$ and $v=0$, and constant heat flux at the wall. The obtained results are presented in Fig. 12.

7.2 Natural Convection. A similar treatment was made by Costa [25] to the natural convection heat transfer problem adjacent to a vertical wall like that presented in Fig. 13. In this case the flow and heat transfer problems are linked, and the solution of both problems need to be obtained simultaneously.

The mass conservation equation is still Eq. (35), and the momentum and energy conservation boundary layer equations are

$$u\frac{\partial v}{\partial x}+v\frac{\partial v}{\partial y}=\nu\frac{\partial^2 v}{\partial x^2}\pm g\beta(T-T_\infty) \tag{54}$$

$$\rho c_P\left(u\frac{\partial T}{\partial x}+v\frac{\partial T}{\partial y}\right)=k\frac{\partial^2 T}{\partial x^2} \tag{55}$$

The plus sign in Eq. (54) applies to the hot wall situation and the minus sign applies to the cold wall situation. Variables are made dimensionless in a different way, and the dimensionless governing parameters are the Prandtl number, Pr, and the Grashof number, $\mathrm{Gr}_Y=g\beta(T_H-T_C)Y^3/\nu^2$, retaining that the characteristic length for natural convection is the wall height, Y.

The similarity variable is defined as

$$\eta=\left(\frac{x}{y}\right)\left(\frac{\mathrm{Gr}_y}{4}\right)^{1/4}\times g_1(\mathrm{Pr}) \tag{56}$$

and the stream function is

$$\psi(x,y)=4\nu\left(\frac{\mathrm{Gr}_y}{4}\right)^{1/4}\times f(\eta)\times g_2(\mathrm{Pr}) \tag{57}$$

where $g_1=[(4\,\mathrm{Pr}^2)/(4+\mathrm{Pr})]^{1/4}$ and $g_2=(\sqrt{2}/2)\mathrm{Pr}^{-1}g_1$ are functions of the Prandtl number, in an attempt to obtain a better fit over the overall Prandtl number range. The dimensionless temperature is defined as

$$\theta[\eta(x,y,\mathrm{Pr})]=\frac{T(x,y)-T_\infty}{|T_w-T_\infty|} \tag{58}$$

The similarity flow and heat transfer problems to solve are

$$f'''=(3ff''-2f'^2)\times(g_2/g_1)(\pm)\theta\times g_1^{-3}g_2^{-1} \tag{59}$$

subjected to $f(0)=f'(0)=0$ and $f'(+\infty)=0$, and

$$\theta''=3\,\mathrm{Pr}\,f\theta'\times(g_2/g_1) \tag{60}$$

subjected to $\theta(0)=(\pm)1$ and $\theta(+\infty)=0$.

The heat function is defined through its first-order derivatives as

$$\frac{\partial H}{\partial y}=\rho u c_p(T-T_c)-k\frac{\partial T}{\partial x} \tag{61a}$$

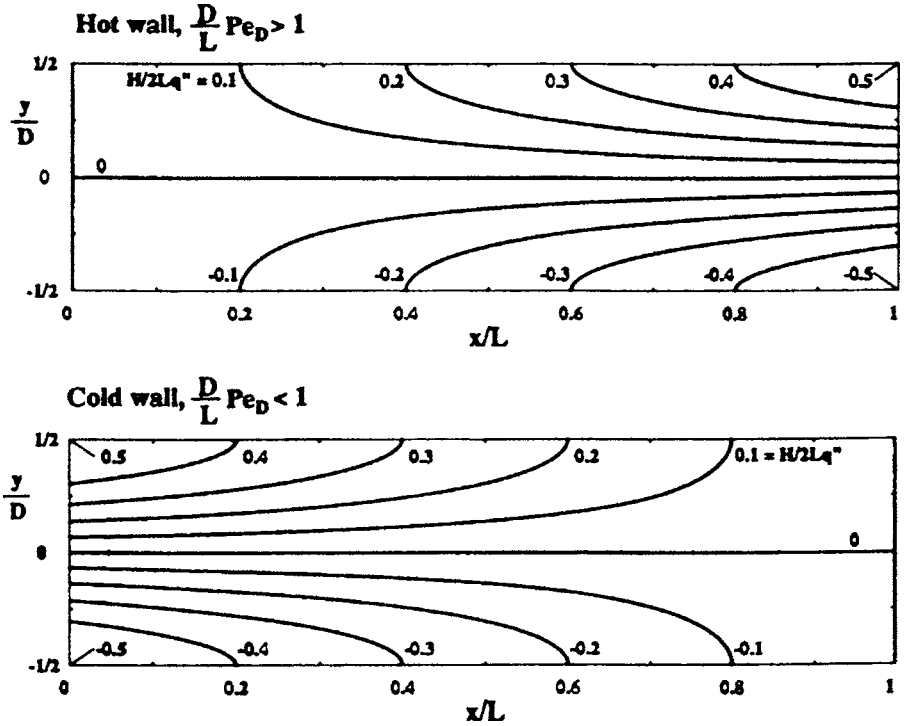

Fig. 12 Heatlines obtained from the analytical solution of the heat function for the forced convection of a pure fluid in slug flow inside a channel. (Top) Near a hot wall and (bottom) near a cold wall (reprinted with permission from [24]).

$$-\frac{\partial H}{\partial x} = \rho v c_p (T - T_c) \tag{61b}$$

The space coordinates are made dimensionless as $y_* = y/Y$ and $x_* = (x/Y)(\mathrm{Gr}_Y/4)^{1/4} \times g_1$, and the similarity variable can be expressed as $\eta(x_*, y_*) = x_* y_*^{-1/4}$. The heat function is made dimensionless as $H_* = H/(k|T_0 - T_\infty|)$.

When the vertical wall is isothermal and hot, the dimensionless similarity solution for the heat function is obtained as

$$H_*(y_*, \eta) = \frac{4}{3}\left(\frac{\mathrm{Gr}_Y}{4}\right)^{1/4} y_*^{3/4}(3\ \mathrm{Pr}\ g_2 f\theta - g_1\theta') \tag{62}$$

When the wall is isothermal and cold the similarity solution for the heat function is

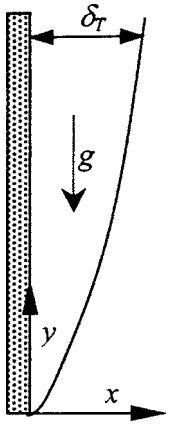

Fig. 13 Boundary layer in natural convection near a vertical flat plate

$$H_*(y_*, \eta) = \frac{4}{3}\left(\frac{\mathrm{Gr}_Y}{4}\right)^{1/4} y_*^{3/4}[3\ \mathrm{Pr}\ g_2 f(\theta - \theta_0) - g_1\theta'] \tag{63}$$

The results obtained by Costa [25] for the heatlines are presented in Figs. 14(*a*) and 14(*b*) for the situations of isothermal hot and cold wall, respectively.

When the hot wall is under constant heat flux, the governing parameters are the Prandtl number, Pr, and the modified Grashof number, $\mathrm{Gr}_y^* = g\beta\dot{q}'' y^4/(kv^2)$, retaining once again that the characteristic length for natural convection is the wall height.

The similarity variable is defined as

$$\eta = \left(\frac{x}{y}\right)\left(\frac{\mathrm{Gr}_y^*}{5}\right)^{1/5} \times g_1(\mathrm{Pr}) \tag{64}$$

and the stream function is

$$\psi(x,y) = 5\nu\left(\frac{\mathrm{Gr}_y^*}{5}\right)^{1/5} \times f(\eta) \times g_2(\mathrm{Pr}) \tag{65}$$

where

$$g_1 = [(5\ \mathrm{Pr}^2)/(7 + \mathrm{Pr})]^{1/5}$$

and $g_2 = (\sqrt{15 \times 7 \times 0.9}/15)\mathrm{Pr}^{-1}\, g_1$ are functions of the Prandtl number, once again in an attempt to obtain a better fit over the overall Prandtl number range. The dimensionless temperature in this case is defined as

$$\theta[\eta(x,y,\mathrm{Pr})] = [T(x,y) - T_\infty]\left(\frac{k}{\dot{q}''}\right)\left(\frac{1}{y}\right)\left(\frac{\mathrm{Gr}_y^*}{5}\right)^{1/5} \times g_1 \tag{66}$$

The similarity flow and heat transfer problems to solve are

$$f''' = (4ff'' - 3f'^2) \times (g_2/g_1)(\pm)\theta \times g_1^{-4} g_2^{-1} \tag{67}$$

subjected to $f(0) = f'(0) = 0$ and $f'(+\infty) = 0$, and

$$\theta'' = \mathrm{Pr}(4f\theta' - f'\theta) \times (g_2/g_1) \tag{68}$$

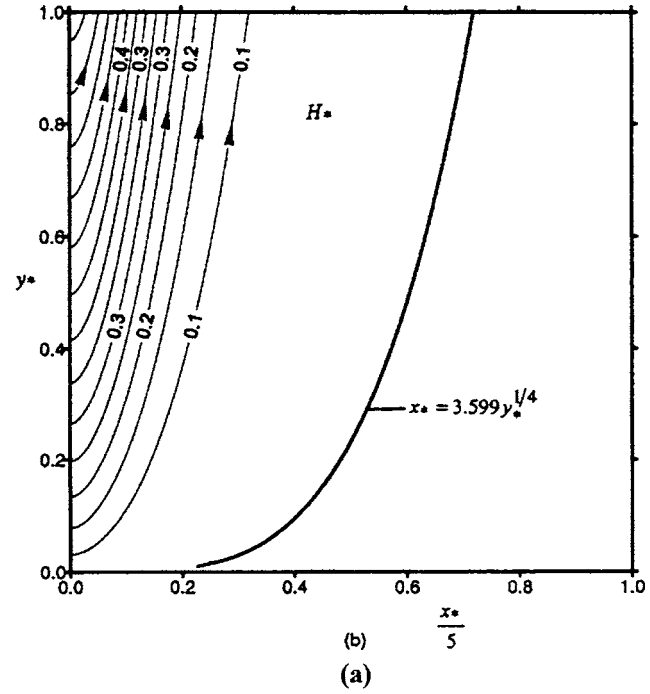

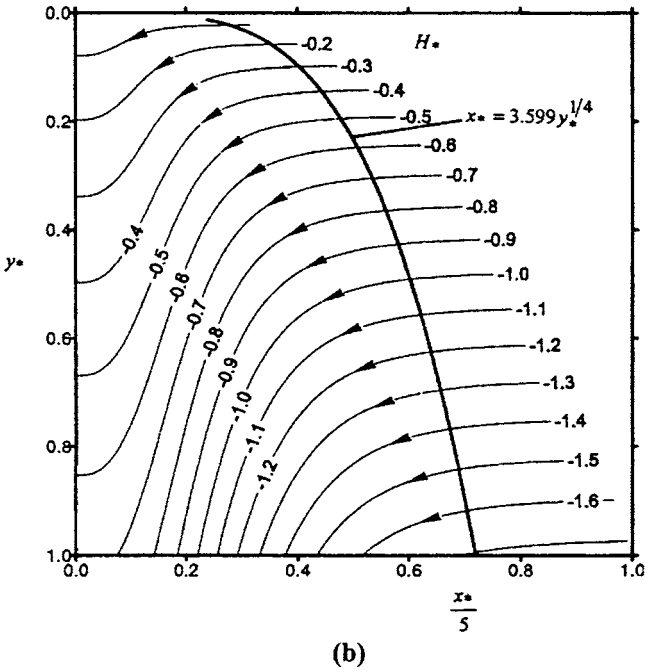

Fig. 14 Heatlines obtained from the similarity solution of the heat function for the natural convection near a vertical isothermal hot flat plate (left) and vertical isothermal cold flat plate (right) (reprinted with permission from [25])

subjected to $\theta'(0)=(\mp)1$ and $\theta(+\infty)=0$.

The heat function is defined through its first-order derivatives by Eqs. (61*a*) and (61*b*), and the space coordinates are now made dimensionless as $y_*=y/Y$ and $x_*=(x/Y)(\mathrm{Gr}_Y^*/5)^{1/5}\times \mathrm{g}_1$, and the similarity variable can be expressed as $\eta(x_*,y_*)=x_* y_*^{-1/5}$. The heat function is made dimensionless as $H_*=H/(\dot{q}''Y)$.

When the vertical wall is hot and under constant wall heat flux, the dimensionless similarity solution for the heatfunction was obtained by Costa [25] as

$$H_*(y_*,\eta)=y_*[4\,\mathrm{Pr}(g_2/g_1)f\theta-\theta'] \tag{69}$$

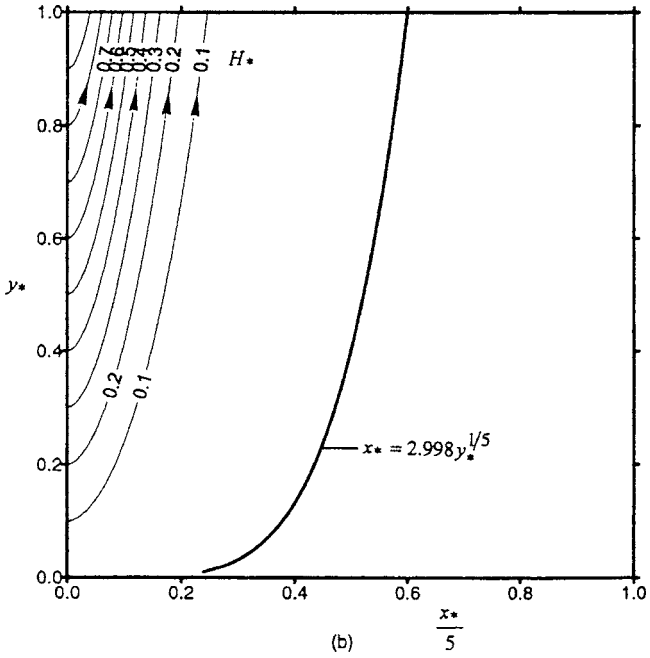

Fig. 15 Heatlines obtained from the similarity solution of the heat function for the natural convection near a vertical hot flat plate under constant wall heat flux (reprinted with permission from [25])

The results obtained by Costa [25] for this situation are presented in Fig. 15. As the vertical wall is under constant heat flux, the heatlines are equally spaced along the height of the vertical wall.

In all the figures, it is evident the importance of the heatlines as visualization tools. The heatlines give a clear and complete picture of the heat transfer processes occurring in the natural convection boundary layers adjacent to vertical walls under different heating or cooling conditions. The existing relationship between the extreme values of the heatfunction and the overall Nusselt number were explored by Costa [25].

It should be noted that the cold wall subjected to a constant heat flux cannot be treated through the similarity solution, as explained by Costa [25].

8 Use of Heatlines in Turbulent Flow

It is well known that when flow takes place in the turbulent regime, additional terms need to be considered into the momentum and energy transport equations. The instantaneous value of each dependent variable is taken as the sum of an average part (in a time sense) and a fluctuation, that is $\tilde{\phi}=\phi+\phi'$, where ϕ is the average value and ϕ' its fluctuation. As the fluctuation is random, its average value is null.

Substituting the instantaneous values of all the dependent variables in the energy conservation equation, Eq. (10), and taking the average over a sufficiently long period yields

$$\frac{\partial}{\partial x}\left[\rho u c_p(T-T_0)-k\frac{\partial T}{\partial x}+\rho c_p\overline{u'(T'-T_0)}\right]+\frac{\partial}{\partial y}\left[\rho v c_p(T-T_0)-k\frac{\partial T}{\partial y}+\rho c_p\overline{v'(T'-T_0)}\right]=0 \tag{70}$$

where it is assumed that the relevant fluctuations occur in the dependent variables u, v, and T. When comparing with the original differential equation, Eq. (10), new terms were introduced by the averaging procedure, which include the crossed relationship between the averaged variables. These additional terms, of the

Table 1 The physical meaning of ϕ, and coupling with Φ, for frequent situations [30].

Physical principle	ϕ	Γ_ϕ	Φ	Φ contour plots
Overall mass conservation	1	0	ψ, stream function	Streamlines
Energy conservation	T	k/c_P	H, heat function	Heatlines
i species mass conservation	C_i	ρD_i	M_i, i species mass function	i species masslines

form $F_i=-\rho c_p\overline{u_i'(T'-T_0)}$, are known as the turbulent fluxes, and they are evaluated using a turbulence model [27].

Once these additional terms are evaluated using an available procedure, the heatfunction in turbulent convective heat transfer can be defined through its first-order derivatives, using Eq. (70), as

$$\frac{\partial H}{\partial y}=\rho u c_p(T-T_0)-k\frac{\partial T}{\partial x}+\rho c_p\overline{u'(T'-T_0)} \tag{71a}$$

$$-\frac{\partial H}{\partial x}=\rho v c_p(T-T_0)-k\frac{\partial T}{\partial y}+\rho c_p\overline{v'(T'-T_0)} \tag{71b}$$

The differential equation for the heatfunction field is evaluated in the same way as for the laminar case, but now using Eqs. (71*a*) and (71*b*), and it results in

$$0=\frac{\partial^2 H}{\partial x^2}+\frac{\partial^2 H}{\partial y^2}+\frac{\partial}{\partial x}[\rho v c_p(T-T_0)+\rho c_p\overline{v'(T'-T_0)}]-\frac{\partial}{\partial y}[\rho u c_p(T-T_0)+\rho c_p\overline{u'(T'-T_0)}] \tag{72}$$

From this point forward, the turbulent situation is treated in the same way as the laminar situation.

Dash [26] used that formulation to obtain the heatlines corresponding to the turbulent heat transfer near a heated vertical plate.

If the heat transfer problem under analysis occurs in the turbulent boundary layer near a wall, the heatline concept can be applied in a simpler way, by using an effective diffusion coefficient for heat. In this case, the heat function is defined through its first-order derivatives as usually for the boundary layer adjacent to a flat plate [27]

$$\frac{\partial H}{\partial y}=\rho u c_p(T-T_0) \tag{73a}$$

$$-\frac{\partial H}{\partial x}=\rho v c_p(T-T_0)-(k+\rho c_p\varepsilon_H)\frac{\partial T}{\partial y} \tag{73b}$$

where the turbulent flux has been expressed as $-\rho c_p\overline{v'(T'-T_0)}=\rho c_p\varepsilon_H(\partial T/\partial y)$. Some results involving the heatlines were obtained by Bejan [27], using such an approach for turbulent boundary layers near hot and cold isothermal walls.

9 Unification of the Streamline, Heatline, and Massline Methods

The streamline, heatline, and massline methods were unified by Costa [30], in order to be subjected to a common treatment, and in order to be easily included, through a common procedure, into CFD packages.

The differential conservation equation for the general variable F, whose specific value is $\phi=F/m$, can be written as

$$\frac{\partial}{\partial x}\left[\rho u(\phi-\phi_0)-\Gamma_\phi\frac{\partial\phi}{\partial x}\right]+\frac{\partial}{\partial y}\left[\rho v(\phi-\phi_0)-\Gamma_\phi\frac{\partial\phi}{\partial y}\right]=0 \tag{74}$$

where ϕ_0 is a reference value for ϕ, taken as its lower value in the entire domain under analysis. In Eq. (74) are identified the flux components of the total flux $\mathbf{J}_\phi$ as

$$J_{\phi,x}=\rho u(\phi-\phi_0)-\Gamma_\phi\frac{\partial\phi}{\partial x} \tag{75a}$$

$$J_{\phi,y}=\rho v(\phi-\phi_0)-\Gamma_\phi\frac{\partial\phi}{\partial y} \tag{75b}$$

Function $\Phi(x,y)$, associated with the variable ϕ, and whose contour plots will be used for visualization and analysis purposes, is defined through its first order derivatives as

$$\frac{\partial\Phi}{\partial y}=\rho u(\phi-\phi_0)-\Gamma_\phi\frac{\partial\phi}{\partial x} \tag{76a}$$

$$-\frac{\partial\Phi}{\partial x}=\rho v(\phi-\phi_0)-\Gamma_\phi\frac{\partial\phi}{\partial y} \tag{76b}$$

Equation (74) can be identically obtained by equating the second order crossed derivatives of Φ evaluated from Eqs. (76*a*) and (76*b*), being implicitly assumed that $\Phi(x,y)$ is a continuous function to its second order derivatives.

Assuming now that ϕ is a continuous function to its second order derivatives, one can establish the equality of its second order crossed derivatives through the expressions obtained from the right-hand sides of Eqs. (76*a*) and (76*b*), leading to

$$0=\frac{\partial}{\partial x}\left(\frac{1}{\Gamma_\phi}\frac{\partial\Phi}{\partial x}\right)+\frac{\partial}{\partial y}\left(\frac{1}{\Gamma_\phi}\frac{\partial\Phi}{\partial y}\right)+\left\{\frac{\partial}{\partial x}\left[\frac{\rho v}{\Gamma_\phi}(\phi-\phi_0)\right]-\frac{\partial}{\partial y}\left[\frac{\rho u}{\Gamma_\phi}(\phi-\phi_0)\right]\right\} \tag{77}$$

This is the second-order partial differential equation (a Poisson equation) from which it is evaluated in the Φ field, for any particular corresponding meaning of ϕ. It is an equation corresponding to a conduction-type problem, with source term if the fluid flow subsists, and without source term if the fluid flow subsides, with the diffusion coefficient for Φ verifying

$$\Gamma_\Phi=1/\Gamma_\phi \tag{78}$$

The diffusion coefficient $\Gamma_\Phi=1/\Gamma_\phi$ is maintained within parentheses in Eq. (77) because it is, in the general case, a variable and not a constant. To the author's knowledge, this was the first formulation considering a variable diffusion coefficient for Φ.

For $\phi=1$, $\phi_0=0$, and $\Gamma_\phi=\varepsilon$, a small constant number, one obtains the well-known partial differential equation for the stream function, Eq. (5). The particular meaning of ϕ and its respective Φ, whose contour plots are used for visualization and analysis purposes, for some usual situations, are summarized in Table 1.

In what concerns the boundary conditions for Eq. (77), they can be specified as

$$\Phi(x_{\text{ref}},y)=\Phi(x_{\text{ref}},y_{\text{ref}})+\int_{y_{\text{ref}}}^{y}\left[\rho u(\phi-\phi_0)-\Gamma_\phi\frac{\partial\phi}{\partial x}\right]dy \quad (79)$$

along a boundary with constant x, or as

$$\Phi(x,y_{\text{ref}})=\Phi(x_{\text{ref}},y_{\text{ref}})-\int_{x_{\text{ref}}}^{x}\left[\rho v(\phi-\phi_0)-\Gamma_\phi\frac{\partial\phi}{\partial y}\right]dx \quad (80)$$

along a boundary with constant y.

Some of the results obtained by Costa [30], for the double-diffusive natural convection in a square enclosure with heat and mass diffusive walls, with opposed buoyancy effects, are presented in Fig. 16.

At the fluid-solid walls interface it is observed as a marked change in the inclination of the heatlines and masslines, which is due to the different heat and mass diffusion coefficients in the fluid and in the solid walls. The so unified streamline, heatline, and massline method can be easily implemented in CFD packages through a common procedure for all the used variables for visualization and analysis.

The definition of the diffusion coefficient for Φ, as given by Eq. (78), generated debate [10]; the work by Costa [31] proving that Eq. (78) is, in fact, the correct equation for the diffusion coefficient of the function Φ used for visualization purposes.

Due to their physical nature, ϕ and Φ must be continuous at the solid-fluid interface. From Fig. 17, at each point of the interface s it is

$$\phi_1=\phi_2 \quad \Phi_1=\Phi_2 \quad (81)$$

The condition that $\Phi_1=\Phi_2$ guarantees the conservation of ϕ through the interface.

At the solid-fluid interface s of Fig. 17, where only the diffusive transfer is present, it is

$$\mathbf{J}_\phi\cdot\mathbf{n}=-\Gamma_\phi\left(\sin\theta\frac{\partial\phi}{\partial x}-\cos\theta\frac{\partial\phi}{\partial y}\right)=-\Gamma_\phi\frac{\partial\phi}{\partial n} \quad (82a)$$

$$\mathbf{J}_\phi\cdot\mathbf{s}=-\Gamma_\phi\left(\cos\theta\frac{\partial\phi}{\partial x}+\sin\theta\frac{\partial\phi}{\partial y}\right)=-\Gamma_\phi\frac{\partial\phi}{\partial s} \quad (82b)$$

The conservation principle of ϕ implies that, at the interface,

$$-\Gamma_{\phi,1}\left(\frac{\partial\phi}{\partial n}\right)_1=-\Gamma_{\phi,2}\left(\frac{\partial\phi}{\partial n}\right)_2 \quad (83)$$

where it is $(\partial\phi/\partial n)_1\neq(\partial\phi/\partial n)_2$ if $\Gamma_{\phi,1}\neq\Gamma_{\phi,2}$.

The counterpart of Eq. (83) for Φ, at the interface, taken as a conserved variable, is

$$-\Gamma_{\Phi,1}\left(\frac{\partial\Phi}{\partial n}\right)_1=-\Gamma_{\Phi,2}\left(\frac{\partial\Phi}{\partial n}\right)_2 \quad (84)$$

Similarly to Eqs. (82*a*) and (82*b*) for ϕ, it can be obtained for Φ that

$$\frac{\partial\Phi}{\partial n}=\sin\theta\frac{\partial\Phi}{\partial x}-\cos\theta\frac{\partial\Phi}{\partial y} \quad (85a)$$

$$\frac{\partial\Phi}{\partial s}=\cos\theta\frac{\partial\Phi}{\partial x}+\sin\theta\frac{\partial\Phi}{\partial y} \quad (85b)$$

Substituting $\partial\Phi/\partial x$ and $\partial\Phi/\partial y$, as given by Eqs. (76*a*) and (76*b*), on the right-hand sides of Eqs. (85*a*) and (85*b*), it results in the most general spatial form of Eqs. (76*a*) and (76*b*) for the sole diffusive situation

$$-\frac{\partial\Phi}{\partial n}=-\Gamma_\phi\frac{\partial\phi}{\partial s} \quad (86a)$$

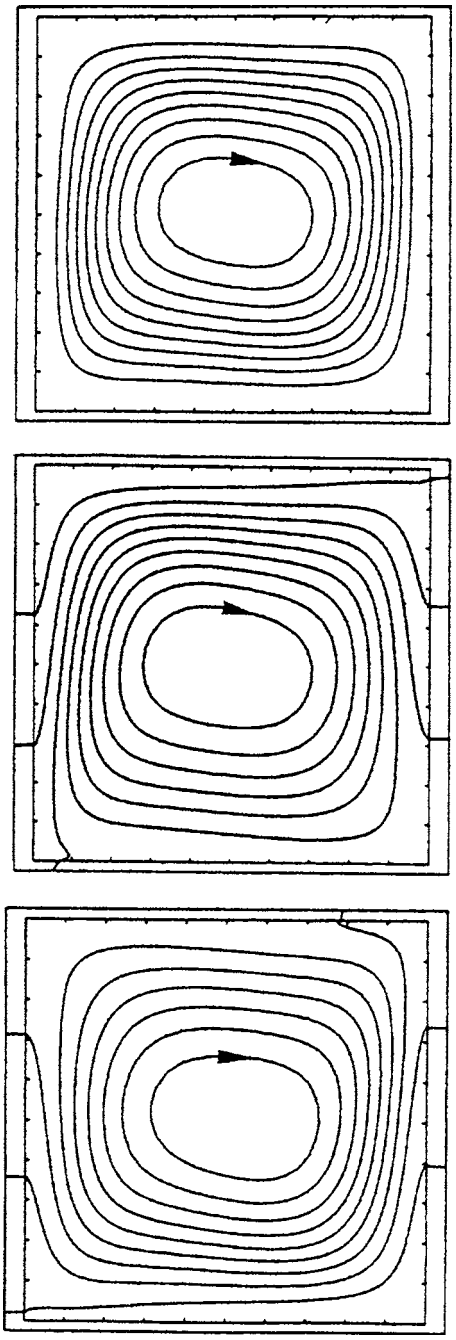

Fig. 16 Streamlines (top), heatlines (center), and masslines (bottom) for the double-diffusive natural convection in a square enclosure with heat and mass diffusive walls, and opposed buoyancy effects (reprinted with permission from [30])

$$\frac{\partial\Phi}{\partial s}=-\Gamma_\phi\frac{\partial\phi}{\partial n} \quad (86b)$$

From Fig. 17 it can be observed that $(\Delta\Phi/\Delta s)_1=(\Delta\Phi/\Delta s)_2$ and that $(\Delta\phi/\Delta s)_1=(\Delta\phi/\Delta s)_2$. In the limit situation, when $\Delta s\to 0$, it results then in

$$\left(\frac{\partial\Phi}{\partial s}\right)_1=\left(\frac{\partial\Phi}{\partial s}\right)_2 \quad (87a)$$

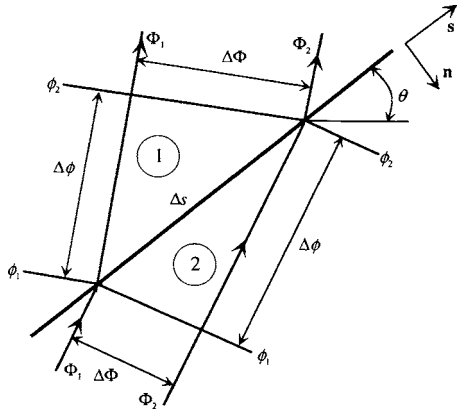

Fig. 17 Lines of constant ϕ and lines of constant Φ, normal to each other at any point, near the interface *s* between media 1 and 2 of different diffusion coefficients (reprinted with permission from [31])

$$\left(\frac{\partial\phi}{\partial s}\right)_1 = \left(\frac{\partial\phi}{\partial s}\right)_2 \tag{87b}$$

Joining together Eqs. (87*b*) and (86*a*), it can be stated that

$$-\frac{1}{\Gamma_{\phi,1}}\left(\frac{\partial\Phi}{\partial n}\right)_1 = -\frac{1}{\Gamma_{\phi,2}}\left(\frac{\partial\Phi}{\partial n}\right)_2 \tag{88}$$

Comparing this result with Eq. (84) it is evident that, in fact, it is $\Gamma_\Phi = 1/\Gamma_\phi$.

The change in direction of the contour plots used for visualization and analysis, due to the existence of adjacent media with different diffusion coefficients, can be referred to as the *refraction* of the heatlines and/or masslines. In fact, a similar situation occurs with the streamlines when analyzing fluid flow in adjacent media of different permeabilities, what is referred to as the refraction of the streamlines in the groundwater bibliography [38,39].

10 Unification of the Streamline, Heatline and Massline Methods for Anisotropic Media

The streamline, heatline, and massline methods have been unified by Costa [32] to apply to anisotropic media, which are of great and increasing practical interest. Recognizing that, in this case, the flux transport components are

$$J_{\phi,x} = \rho u(\phi - \phi_0) - \left[(\Gamma_{\phi,\xi} l_1^2 + \Gamma_{\phi,\eta} l_2^2)\frac{\partial\phi}{\partial x} + (\Gamma_{\phi,\xi} l_1 m_1 + \Gamma_{\phi,\eta} l_2 m_2)\frac{\partial\phi}{\partial y}\right] \tag{89a}$$

$$J_{\phi,y} = \rho v(\phi - \phi_0) - \left[(\Gamma_{\phi,\xi} l_1 m_1 + \Gamma_{\phi,\eta} l_2 m_2)\frac{\partial\phi}{\partial x} + (\Gamma_{\phi,\xi} m_1^2 + \Gamma_{\phi,\eta} m_2^2)\frac{\partial\phi}{\partial y}\right] \tag{89b}$$

where u and v are the area averaged Cartesian velocity components [29], $\Gamma_{\phi,\xi}$ and $\Gamma_{\phi,\eta}$ are the principal diffusion coefficients for ϕ along the ξ,η principal Cartesian directions, which are related with the x,y Cartesian coordinate system through the direction cosines l_1, l_2 and m_1, m_2. With $\Gamma_{\phi,xx} = \Gamma_{\phi,\xi} l_1^2 + \Gamma_{\phi,\eta} l_2^2$, $\Gamma_{\phi,yy} = \Gamma_{\phi,\xi} m_1^2 + \Gamma_{\phi,\eta} m_2^2$, and $\Gamma_{\phi,xy} = \Gamma_{\phi,yx} = \Gamma_{\phi,\xi} l_1 m_1 + \Gamma_{\phi,\eta} l_2 m_2$, Eqs. (89*a*) and (89*b*) become

$$J_{\phi,x} = \rho u(\phi - \phi_0) - \left(\Gamma_{\phi,xx}\frac{\partial\phi}{\partial x} + \Gamma_{\phi,xy}\frac{\partial\phi}{\partial y}\right) \tag{90a}$$

$$J_{\phi,y} = \rho v(\phi - \phi_0) - \left(\Gamma_{\phi,xy}\frac{\partial\phi}{\partial x} + \Gamma_{\phi,yy}\frac{\partial\phi}{\partial y}\right) \tag{90b}$$

Inserting these fluxes into the general conservation equation, it is obtained the general convection-diffusion differential transport equation for ϕ in two-dimensional anisotropic media

$$\frac{\partial}{\partial x}\left[\rho u\phi - \left(\Gamma_{\phi,xx}\frac{\partial\phi}{\partial x} + \Gamma_{\phi,xy}\frac{\partial\phi}{\partial y}\right)\right] + \frac{\partial}{\partial y}\left[\rho v\phi - \left(\Gamma_{\phi,xy}\frac{\partial\phi}{\partial x} + \Gamma_{\phi,yy}\frac{\partial\phi}{\partial y}\right)\right] = 0 \tag{91}$$

When dealing with fluid-saturated anisotropic porous media, the velocity components are usually related to the pressure gradient and the body force (in this case only the gravitational acceleration, being the x,y coordinate system placed such that $g_x = 0$ and $g_y = -g$) through the Darcy flow model, which is sufficiently accurate for many practical applications [29]

$$u = -\frac{1}{\mu}\left[K_{xx}\frac{\partial p}{\partial x} + K_{xy}\left(\frac{\partial p}{\partial y} + \rho g\right)\right] \tag{92a}$$

$$v = -\frac{1}{\mu}\left[K_{xy}\frac{\partial p}{\partial x} + K_{yy}\left(\frac{\partial p}{\partial y} + \rho g\right)\right] \tag{92b}$$

However, if there are interfaces between fluid saturated porous media and pure fluids (the latter governed by the Navier-Stokes equations), or the Reynolds number is high enough such that inertial effects must be taken into account, more detailed and complete models (usually the Brinkman and Forchheimer modifications, respectively) are needed [29].

Different physical meanings of ϕ and its associated transport coefficients can be found in Table 2.

The function $\Phi(x,y)$, whose contour plots are used for visualization purposes, is defined from Eqs. (90*a*) and (90*b*) through its first order derivatives as

Table 2 Physical principles, diffusion coefficients, and source terms for different particular meanings of ϕ [32]

Physical Principle	ϕ	$\Gamma_{\phi,xx}$	$\Gamma_{\phi,yy}$	$\Gamma_{\phi,xy}$	S_ϕ
Overall mass conservation	1	0	0	0	0
i species mass conservation	C_i	$\rho D_{i,xx}$	$\rho D_{i,yy}$	$\rho D_{i,xy}$	0
Energy conservation	T	k_{xx}/c_P	k_{yy}/c_P	k_{xy}/c_P	0
Overall mass conservation (Darcy flow model)	p	$\rho K_{xx}/\mu$	$\rho K_{yy}/\mu$	$\rho K_{xy}/\mu$	$\frac{\partial}{\partial x}\left(\frac{\rho^2 g K_{xy}}{\mu}\right) + \frac{\partial}{\partial y}\left(\frac{\rho^2 g K_{yy}}{\mu}\right)$

Table 3 Coupling of ϕ and Φ and the diffusion coefficients for Φ for some usual situations [32]

Physical principle	ϕ	Φ	$\Gamma_{\Phi,xx}$	$\Gamma_{\Phi,yy}$	$\Gamma_{\Phi,xy}$	Φ contour plots
Overall mass conservation	1	ψ stream function	$\frac{\mu K_{xx}}{\rho K^2}$	$\frac{\mu K_{yy}}{\rho K^2}$	$\frac{\mu K_{xy}}{\rho K^2}$	Streamlines
i species mass conservation	C_i	M_i, i species mass function	$\frac{D_{i,xx}}{\rho D_i^2}$	$\frac{D_{i,yy}}{\rho D_i^2}$	$\frac{D_{i,xy}}{\rho D_i^2}$	i species masslines
Energy conservation	T	H, heat function	$\frac{c_p k_{xx}}{k^2}$	$\frac{c_p k_{yy}}{k^2}$	$\frac{c_p k_{xy}}{k^2}$	Heatlines

$K^2=K_{xx}K_{yy}-K_{xy}^2$, $D_i^2=D_{i,xx}D_{i,yy}-D_{i,xy}^2$, and $k^2=k_{xx}k_{yy}-k_{xy}^2$

$$\frac{\partial\Phi}{\partial y}=J_{\phi,x}=\rho u(\phi-\phi_0)-\left[\Gamma_{\phi,xx}\frac{\partial\phi}{\partial x}+\Gamma_{\phi,xy}\frac{\partial\phi}{\partial y}\right] \quad (93a)$$

$$-\frac{\partial\Phi}{\partial x}=J_{\phi,y}=\rho v(\phi-\phi_0)-\left[\Gamma_{\phi,xy}\frac{\partial\phi}{\partial x}+\Gamma_{\phi,yy}\frac{\partial\phi}{\partial y}\right] \quad (93b)$$

Equating the second-order mixed derivatives of Φ, being implicitly assumed that it is a continuous function to its second order derivatives, Eq. (91) is identically obtained.

From Eqs. (93*a*) and (93*b*) it can be obtained that

$$\frac{\partial\phi}{\partial x}=-\frac{\Gamma_{\phi,yy}}{\Gamma^2}\frac{\partial\Phi}{\partial y}-\frac{\Gamma_{\phi,xy}}{\Gamma^2}\frac{\partial\Phi}{\partial x}+\frac{\Gamma_{\phi,yy}}{\Gamma^2}\rho u(\phi-\phi_0)-\frac{\Gamma_{\phi,xy}}{\Gamma^2}\rho v(\phi-\phi_0) \quad (94a)$$

$$\frac{\partial\phi}{\partial y}=\frac{\Gamma_{\phi,xx}}{\Gamma^2}\frac{\partial\Phi}{\partial x}-\frac{\Gamma_{\phi,xy}}{\Gamma^2}\frac{\partial\Phi}{\partial y}+\frac{\Gamma_{\phi,xx}}{\Gamma^2}\rho v(\phi-\phi_0)-\frac{\Gamma_{\phi,xy}}{\Gamma^2}\rho u(\phi-\phi_0) \quad (94b)$$

where

$$\Gamma^2=\Gamma_{\phi,xx}\Gamma_{\phi,yy}-\Gamma_{\phi,xy}^2 \quad (>0) \quad (95)$$

Assuming now that ϕ is a continuous function to its second order derivatives, it can be established that the equality of its second order crossed derivatives, obtained from Eqs. (94*a*) and (94*b*), lead to the equation

$$\begin{aligned}0=&\frac{\partial}{\partial x}\left(\frac{\Gamma_{\phi,xx}}{\Gamma^2}\frac{\partial\Phi}{\partial x}\right)+\frac{\partial}{\partial y}\left(\frac{\Gamma_{\phi,yy}}{\Gamma^2}\frac{\partial\Phi}{\partial y}\right)+\left[\frac{\partial}{\partial x}\left(\frac{\Gamma_{\phi,xy}}{\Gamma^2}\frac{\partial\Phi}{\partial y}\right)\right.\\&\left.+\frac{\partial}{\partial y}\left(\frac{\Gamma_{\phi,xy}}{\Gamma^2}\frac{\partial\Phi}{\partial x}\right)\right]+\frac{\partial}{\partial x}\left[\frac{\rho(\phi-\phi_0)}{\Gamma^2}(\Gamma_{\phi,xx}v-\Gamma_{\phi,xy}u)\right]\\&-\frac{\partial}{\partial y}\left[\frac{\rho(\phi-\phi_0)}{\Gamma^2}(\Gamma_{\phi,yy}u-\Gamma_{\phi,xy}v)\right]\end{aligned} \quad (96)$$

This is the diffusion equation for Φ in anisotropic media, with the source term present in the second and third rows. It is evident from Eq. (96) that the diffusion coefficients for Φ in anisotropic media are

$$\Gamma_{\Phi,xx}=\frac{\Gamma_{\phi,xx}}{\Gamma^2} \quad \Gamma_{\Phi,yy}=\frac{\Gamma_{\phi,yy}}{\Gamma^2} \quad \Gamma_{\Phi,xy}=\frac{\Gamma_{\phi,xy}}{\Gamma^2} \quad (97)$$

If the x,y coordinate system is coincident with the principal system, it is $\Gamma_{\Phi,xx}=\Gamma_{\Phi,\xi}=1/\Gamma_{\phi,\eta}$ and $\Gamma_{\Phi,yy}=\Gamma_{\Phi,\eta}=1/\Gamma_{\phi,\xi}$, i.e., the principal diffusion coefficients for Φ are the inverse of the diffusion coefficient for ϕ in the perpendicular directions. For isotropic media, it comes that $\Gamma_\Phi=1/\Gamma_\phi$, as given by Eq. (78).

Similarly to what was made to obtain the differential equation for Φ, defining the stream function ψ (overall mass function) through its first order derivatives as given by Eqs. (2*a*) and (2*b*) it is obtained the diffusion equation for ψ in anisotropic media,

$$\begin{aligned}0=&\frac{\partial}{\partial x}\left(\frac{\mu K_{xx}}{\rho K^2}\frac{\partial\psi}{\partial x}\right)+\frac{\partial}{\partial y}\left(\frac{\mu K_{yy}}{\rho K^2}\frac{\partial\psi}{\partial y}\right)+\left[\frac{\partial}{\partial x}\left(\frac{\mu K_{xy}}{\rho K^2}\frac{\partial\psi}{\partial y}\right)\right.\\&\left.+\frac{\partial}{\partial y}\left(\frac{\mu K_{xy}}{\rho K^2}\frac{\partial\psi}{\partial x}\right)\right]-\frac{\partial}{\partial x}(\rho g)\end{aligned} \quad (98)$$

where $K^2=K_{xx}K_{yy}-K_{xy}^2$, which is formally similar to Eq. (96). It is evident that the diffusion coefficients for ψ are

$$\Gamma_{\psi,xx}=\frac{\mu K_{xx}}{\rho K^2} \quad \Gamma_{\psi,yy}=\frac{\mu K_{yy}}{\rho K^2} \quad \Gamma_{\psi,xy}=\frac{\mu K_{xy}}{\rho K^2} \quad (99)$$

The most common meaning of ϕ and its associated Φ function used for visualization and analysis purposes is summarized in Table 3.

In what concerns the boundary conditions for variable Φ, they can be stated as

$$\Phi_{P,B}=\Phi_{\mathrm{ref},B}+\int_{\mathrm{ref},B}^{P,B}\mathbf{J}_\phi\cdot\mathbf{n}\mathrm{d}s_B \quad (100)$$

Due to their physical nature, ϕ and Φ are C^0 continua. Thus, at each point of any interface between contiguous portions 1 and 2 of the domain, even with different properties (as it is the case of conjugate heat and/or mass transfer problems), it is

$$\phi_1=\phi_2 \quad (101a)$$

$$\Phi_1=\Phi_2 \quad (101b)$$

Also due to its physical nature, $\Phi_1=\Phi_2$ (or $\psi_1=\psi_2$) guarantees the conservation of ϕ through such an interface.

This unified method has been successfully applied to some selected problems by Costa [32], and some of the obtained results for the configuration presented in Fig. 18 are presented in Fig. 19.

From this figure the rich picture given by the heatlines about the heat transfer process is clear. It is also clear that the unified method can be easily used to obtain, in a common basis, the streamlines, the heatlines and, eventually, the masslines. The unified method can be easily incorporated into CFD software packages, and the case of isotropic media is just a particular case of the general method as developed to apply to anisotropic media.

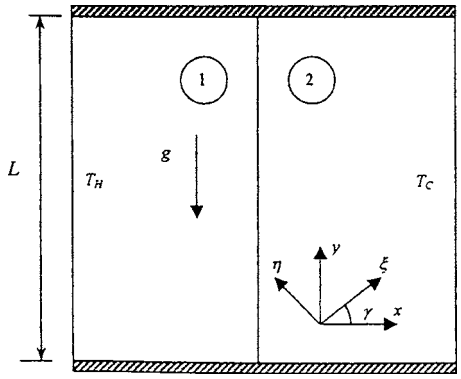

Fig. 18 Physical model and geometry for the analyzed problems involving anisotropic media. The left and right parts of the domain are under different conditions, and they have different properties (reprinted with permission from [32]).

11 Extension and Unification of the Heatline and Massline Concepts to Reacting Flows

The heatline and massline concepts were also extended to be applied to reacting flows. As such methods apply to situations without source terms (divergence-free problems), special care needs to be taken when selecting the variables used for visualization.

In the work of Mukhopadhyay et al. [33], the selected conserved scalars used for visualization and analysis are the elemental mass fractions of the involved chemical species, and the total enthalpy (enthalpy of reaction plus sensible enthalpy). Special (and involved) forms of the conservation equations and of their transport coefficients need to be taken. In a more recent work Mukhopadhyay et al. [34] presented a unified heatline and massline formulation to deal with reacting flows, using the same scalars for visualization, which is summarized here.

The equations for conservation of species and energy can be written, respectively, as

$$\frac{\partial}{\partial r}\left[r^p \rho v_r Z_j - r^p\left(\rho \sum_i D_{i-N_2} w_{i,j} \frac{\partial Y_i}{\partial r}\right)\right] + \frac{\partial}{\partial z}\left[r^p \rho v_z Z_j - r^p\left(\rho \sum_i D_{i-N_2} w_{i,j} \frac{\partial Y_i}{\partial z}\right)\right] = 0 \tag{102}$$

$$\frac{\partial}{\partial r}\left[r^p \rho v_r h - r^p\left(k\frac{\partial T}{\partial r} + \rho \sum_i D_{i-N_2} h_i \frac{\partial Y_i}{\partial r}\right)\right] + \frac{\partial}{\partial z}\left[r^p \rho v_z h - r^p\left(k\frac{\partial T}{\partial z} + \rho \sum_i D_{i-N_2} h_i \frac{\partial Y_i}{\partial z}\right)\right] = 0 \tag{103}$$

where $p=0$ in the case of Cartesian coordinates, and $p=1$ in the case of cylindrical coordinates.

In the search of a unified method, the differential conservation equations are written in a common form as

$$\frac{\partial}{\partial r}\left(r^p \rho v_r \phi - r^p \Gamma_\phi \frac{\partial \phi}{\partial r}\right) + \frac{\partial}{\partial z}\left(r^p \rho v_z \phi - r^p \Gamma_\phi \frac{\partial \phi}{\partial z}\right) + r^p\left(\frac{\partial S_r}{\partial r} + \frac{\partial S_z}{\partial z}\right) = 0 \tag{104}$$

The specific forms of ϕ, Γ_ϕ, S_r, and S_z are presented in Table 4. Making use of the global mass conservation, Eq. (104) can be rewritten as

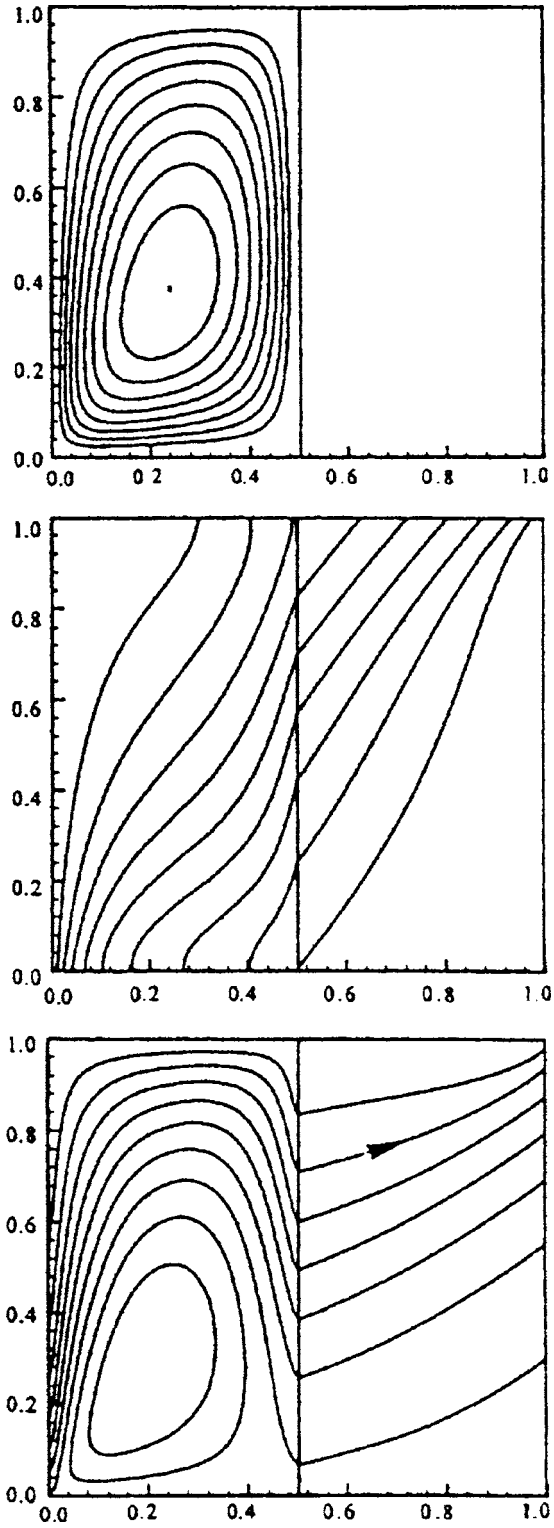

Fig. 19 Streamlines (top), isotherms (center), and heatlines (bottom), for natural convection in a rectangular porous enclosure (left-half of the domain) and pure conduction on the right-half of the domain, for different properties and anisotropic characteristics of the involved media (reprinted with permission from [32])

$$\frac{\partial}{\partial r}\left\{ r^p\left[\rho v_r(\phi - \phi_{\text{ref}}) - \Gamma_\phi \frac{\partial \phi}{\partial r} + S_r\right]\right\} + \frac{\partial}{\partial z}\left\{ r^p\left[\rho v_z(\phi - \phi_{\text{ref}}) - \Gamma_\phi \frac{\partial \phi}{\partial z} + S_z\right]\right\} = 0 \tag{105}$$

Table 4 Scalar functions for visualization of mass, energy, and species transport [34]

Function	Φ	ϕ	Γ_ϕ	S_r	S_z
Stream function	ψ	1	0	0	0
Elemental mass function	M_j	$Z_j = W_j \sum_i \frac{\mu_{j,i} Y_i}{MW_i}$	ρD_{1-N_2}	$\rho \sum_{\substack{i \\ i \neq 1}} (D_{1-N_2} - D_{i-N_2}) w_{j,i} \frac{\partial Y_i}{\partial r}$	$\rho \sum_{\substack{i \\ i \neq 1}} (D_{1-N_2} - D_{i-N_2}) w_{j,i} \frac{\partial Y_i}{\partial z}$
Enthalpy function	H	$H = \sum_i Y_i (\Delta h_{f,i} + \int_{T_{\text{ref}}}^{T} c_{p,i} dT)$	k/c_p	$\sum_i \left(\frac{k}{c_p} - \rho D_{i-N_2} \right) \frac{\partial Y_i}{\partial r}$	$\sum_i \left(\frac{k}{c_p} - \rho D_{i-N_2} \right) \frac{\partial Y_i}{\partial z}$

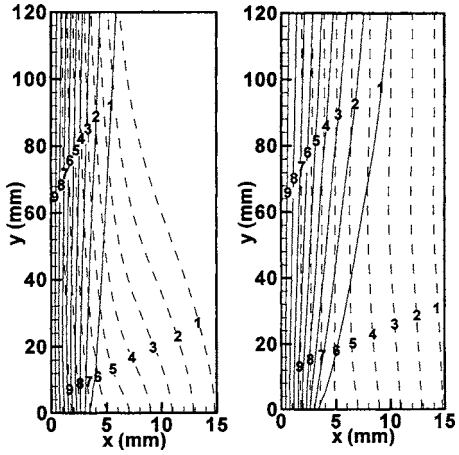

Fig. 20 Enthalpy lines (solid lines) and streamlines (dashed lines) for a planar hot jet of air issuing into an ambient at lower velocity, under normal gravity conditions (left) and absent gravity conditions (right) (reprinted with permission from [34])

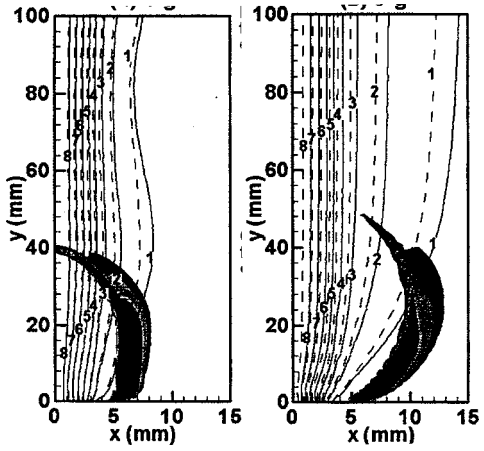

Fig. 21 Mixture fraction lines for nonpremixed planar methane-air jet flames superposed on heat release rate contours, under normal gravity (left), and absent gravity (right). Solid lines for the H element, and dotted lines for the C element. The heat release contours enable the finding of the position of the flame (reprinted with permission from [34]).

From that equation it can be identified the flux components of the conserved variable ϕ. Its counterpart, Φ, used for visualization and analysis purposes can then be defined through its first-order derivatives as

$$\frac{\partial \Phi}{\partial z} = r^p \left[\rho v_r (\phi - \phi_{\text{ref}}) - \Gamma_\phi \frac{\partial \phi}{\partial r} + S_r \right] \tag{106a}$$

$$-\frac{\partial \Phi}{\partial r} = r^p \left[\rho v_z (\phi - \phi_{\text{ref}}) - \Gamma_\phi \frac{\partial \phi}{\partial z} + S_z \right] \tag{106b}$$

Equation (105) can be identically obtained by equating the second order crossed derivatives of Φ, assuming that it is a function continuous to its second order derivatives.

Mukhopadhyay et al. [34] obtained results both for nonreacting and for reacting flows, some of which are presented below. In Fig. 20 are presented the results, in the form of enthalpy lines and streamlines, corresponding to a planar hot air jet issuing into an ambient at a lower velocity, under normal or absent gravity conditions. Results for reacting flows, for a nonpremixed methane-air flame, established in a slot burner, under normal or absent gravity conditions, are presented in Fig. 21.

The presented results clearly show the high potential of the heatline and massline methods to also apply to reacting flows. The unified method, as proposed by Mukhopadhyay et al. [34], can be easily incorporated into CFD packages, with the possibility of dealing with both nonreacting or reacting flows. The case of nonreacting flows is only a simple case of the more general formulation.

12 Conclusions

Heatlines and masslines are, in fact, the most adequate tools for visualization and analysis of two-dimensional convective heat and/or mass transfer. They give the paths followed by energy and/or mass, which is a picture that cannot be directly obtained from the isotherms and/or isoconcentration lines in convection problems.

When made properly dimensionless, the numerical values of the heat function and/or mass function are closely related to the overall Nusselt and/or Sherwood numbers, which characterize the overall heat and/or mass transfer processes.

The method was invented two decades ago. It has evolved, and is now mature and ready to be used as a systematic analysis tool. The streamline, heatline, and massline methods can be treated through common procedures, which can be easily implemented in CFD packages, both for convective heat and/or mass transfer in isotropic or in anisotropic media. The last is the application of the method to reacting flows, which considerably enlarges the applicability range of these useful tools.

Nomenclature

A = surface area
C = mass fraction
c_p = constant pressure specific heat
D = channel width
D = diffusion coefficient
$D_{i\text{–}N_2}$ = binary diffusion coefficient of species i in N_2
f = similarity function
g = auxiliary function
g = gravitational acceleration
grad = gradient vector
Gr = grashof number
h = mixture enthalpy
h_i = enthalpy of species i
H = heat function
$\mathbf{i},\mathbf{j}$ = unit Cartesian vectors
$\mathbf{J}_e$ = energy flux vector
$\mathbf{J}_m$ = mass flux vector
$\mathbf{J}_{m,i}$ = mass flux vector of chemical species i
$\mathbf{J}_\phi$ = flux vector of ϕ
k = thermal conductivity
K = permeability
l,m = director cosines
L = length
Le = Lewis number
M = mass function
$\dot{m}$ = mass flow rate
$\mathbf{n}$ = outward normal unit vector
N = buoyancy factor
Nu = Nusselt number
p = pressure
Pe = Péclet number
Pr = Prandtl number
$\dot{q}''$ = heat flux
$\dot{Q}$ = heat flow
r = radial coordinate (radial and spherical systems)
Ra = Rayleigh number
Re = Reynolds number
s = length segment
S = source term
t = time
T = temperature
U = free stream or mean velocity
u,v = Cartesian velocity components
$w_{i,j}$ = number of atoms of element element j in species i
x,y = Cartesian coordinates
Y = mass fraction
Y = total height
z = longitudinal coordinate
Z = elemental mass fraction

Greek Symbols

α = thermal diffusivity
β = volumetric expansion coefficient
Γ = diffusion coefficient
Δ = difference value
δ = boundary layer thickness
ε_H = eddy diffusivity for heat
ξ,η = principal directions
η = similarity variable
θ = tangential coordinate (cylindrical system)
θ = azimuthal coordinate (spherical system)
θ = dimensionless temperature
μ = dynamic viscosity
μ_{ji} = number of atoms of element j in 1 molecule of species i
ν = kinematic viscosity
ρ = density
ϕ = generic variable
Φ = generic variable, used for visualization
ψ = stream function

Subscripts

B = at the boundary
C = cold wall
H = hot wall
i = Chemical species i
L = based on length L
Q = heat conduction
r = radial
ref = reference point or reference value
T = thermal boundary layer
w = at the wall
xx = tensor component in the x direction
xy = crossed tensor component
yy = tensor component in the y direction
Y = based on height Y
z = longitudinal direction
θ = tangential or azimuthal direction
ϕ = generic variable
Φ = generic variable
0 = reference value
∞ = free stream value
* = dimensionless

Superscripts

p = index for coordinate system shifting

References

[1] White, F. M., 1977, *Viscous Fluid Flow*, 2nd ed., McGraw-Hill, New York, p. 62.
[2] Eckert, E. R. G., and Drake, R. M. Jr., 1972, *Analysis of Heat and Mass Transfer*, McGraw-Hill, New York, Chap. 1.
[3] Kimura, S., and Bejan, A., 1983, "The Heatline Visualization of Convective Heat Transfer," ASME J. Heat Transfer, **105**, pp. 916–919.
[4] Bejan, A., 1984, *Convection Heat Transfer*, Wiley, New York, pp. 21–23.
[5] Trevisan, O. V., and Bejan, A., 1987, "Combined Heat and Mass Transfer by Natural Convection in a Vertical Enclosure," ASME J. Heat Transfer, **109**, pp. 104–112.
[6] Bello-Ochende, F. L., 1987, "Analysis of Heat Transfer by Free Convection in Tilted Rectangular Cavities Using the Energy-Analogue of the Stream Function," Int. J. Mech. Eng. Education, **15**(2), pp. 91–98.
[7] Bello-Ochende, F. L., 1988, "A Heat Function Formulation for Thermal Convection in a Square Cavity," Int. Commun. Heat Mass Transfer, **15**, pp. 193–202.
[8] Oh, J. Y., Ha, M. Y., and Kim, K. C., 1997, "Numerical Study of Heat Transfer and Flow of Natural Convection in an Enclosure With Heat-Generating Conducting Body," Numer. Heat Transfer, Part A, **31**, pp. 289–303.
[9] Costa, V. A. F., 1997, "Double-Diffusive Natural Convection in a Square Enclosure With Heat and Mass Diffusive Walls," Int. J. Heat Mass Transfer, **40**(17), pp. 4061–4071.
[10] Deng, Q.-H., and Tang, G.-F., 2002, "Numerical Visualization of Mass and Heat Transport for Conjugate Natural Convection/Heat Conduction by Streamline and Heatline," Int. J. Heat Mass Transfer, **45**(11), pp. 2375–2385.
[11] Deng, Q.-H., and Tang, G.-F., 2002, "Numerical Visualization of Mass and Heat Transport for Mixed Convective Heat Transfer by Streamline and Heatline," Int. J. Heat Mass Transfer, **45**(11), pp. 2387–2396.
[12] Deng, Q.-H., Tang, G.-F., and Li, Y., 2002, "A Combined Temperature Scale for Analyzing Natural Convection in Rectangular Enclosures With Discrete Heat Sources," Int. J. Heat Mass Transfer, **45**(16), pp. 3437–3446.
[13] Costa, V. A. F., 2004, "Double-Diffusive Natural Convection in Parallelogrammic Enclosures Filled With Fluid-Saturated Porous Media," Int. J. Heat Mass Transfer, **47**(12–13), pp. 2699–2714.
[14] Morega, Al-M., 1988, "Magnetic Field Influence on the Convective Heat Transfer in the Solidification Processes, Part 2," Rev. Roum. Sci. Tech.-Electrotech. et Energ., **33**(2), pp. 155–166.
[15] Morega, Al-M., 1988, "The Heat Function Approach to the Thermomagnetic Convection of Electroconductive Melts," Rev. Roum. Sci. Tech.-Electrotech. et Energ., **33**(4), pp. 359–368.
[16] Aggarwal, S. K., and Manhapra, A., 1989, "Use of Heatlines for Unsteady Buoyancy-Driven Flow in a Cylindrical Enclosure," ASME J. Heat Transfer, **111**, pp. 576–578.
[17] Aggarwal, S. K., and Manhapra, A., 1989, "Transient Natural Convection in a Cylindrical Enclosure Nonuniformly Heated at the Top Wall," Numer. Heat

Transfer, Part A, **15**, pp. 341–356.
[18] Littlefield, D., and Desai, O., 1986, "Buoyant Laminar Convection in a Vertical Cylindrical Annulus," ASME J. Heat Transfer, **108**, pp. 814–821.
[19] Ho, C. J., and Lin, Y. H., 1989, "Thermal Convection Heart Transfer of Air/Water Layers Enclosed in Horizontal Annuli With Mixed Boundary Conditions," Waerme- Stoffuebertrag., **24**, pp. 211–224.
[20] Ho, C. J., Lin, Y. H., Chen, T. C., 1989, "A Numerical Study of Natural Convection in Concentric and Eccentric Horizontal Cylindrical Annuli With Mixed Boundary Conditions," Int. J. Heat Fluid Flow, **10**(1), pp. 40–47.
[21] Ho, C. J., and Lin, Y. H., 1990, "Natural Convection of Cold Water in a Vertical Annulus With Constant Heat Flux on the Inner Wall," ASME J. Heat Transfer, **112**, pp. 117–123.
[22] Chattopadhyay, H., and Dash, S. K., 1995, "Numerical Visualization of Convective Heat Transfer From a Sphere-With and Without Radial Mass Efflux," Int. J. Numer. Methods Heat Fluid Flow, **5**, pp. 705–716.
[23] Morega, Al. M., and Bejan, A., 1993, "Heatline Visualization of Forced Convection Laminar Boundary Layers," Int. J. Heat Mass Transfer, **36**(16), pp. 3957–3966.
[24] Morega, Al. M., and Bejan, A., 1994, "Heatline Visualization of Forced Convection in Porous Media," Int. J. Heat Fluid Flow, **15**(1), pp. 42–47.
[25] Costa, V. A. F., 2000, "Heatline and Massline Visualization of the Laminar Natural Convection Boundary Layers Near a Vertical Wall," Int. J. Heat Mass Transfer, **43**(20), pp. 3765–3774.
[26] Dash, S. K., 1996, "Heatline Visualization in Turbulent Flow," Int. J. Numer. Methods Heat Fluid Flow, **5**(4), pp. 37–46.
[27] Bejan, A., 1995, *Convection Heat Transfer*, 2nd ed., Wiley, New York.
[28] Bejan, A., 2004, *Convection Heat Transfer*, 3rd ed., Wiley, New York.
[29] Nield, D. A., and Bejan, A., 1999, *Convection in Porous Media*, 2nd ed., Springer, New York.
[30] Costa, V. A. F., 1999, "Unification of the Streamline, Heatline and Massline Methods for the Visualization of Two-Dimensional Transport Phenomena," Int. J. Heat Mass Transfer, **42**(1), pp. 27–33.
[31] Costa, V. A. F., 2003, "Comment on the Paper by Qi-Hong Deng, Guang-Fa Tang, Numerical Visualization of Mass and Heat Transport for Conjugate Natural Convection/Heat Conduction by Streamline and Heatline," IJHMT 2002 45 (11) 2373-2385, Int. J. Heat Mass Transfer, **46**(1), pp. 185–187.
[32] Costa, V. A. F., 2003, "Unified Streamline, Heatline and Massline Methods for the Visualization of Two-Dimensional Heat and Mass Transfer in Anisotropic Media," Int. J. Heat Mass Transfer, **46**(8), pp. 1309–1320.
[33] Mukhopadhyay, A., Qin, X., Aggarwal, and S. K., and Puri, I. K., 2002, "On Extension of Heatline and Massline Concepts to Reacting Flows Through Use of Conserved Scalars," ASME J. Heat Transfer, **124**, pp. 791–799.
[34] Mukhopadhyay, A., Qin, X., Puri, I. K., and Aggarwal, S. K., 2003, "Visualization of Scalar Transport in Nonreacting and Reacting Jets Through a Unified Heatline and Massline Formulation," Numer. Heat Transfer, Part A, **44**, pp. 683–704.
[35] Costa, V. A. F., 2004, "Visualization of Two-Dimensional Heat and Mass Transfer Using the Heatlines and Masslines," in *Proceedings of the Symposium Bejan's Constructal Theory of Shape and Structure*, R. N. Rosa, A. H. Reis, A. F. Miguel, eds., Évora Geophysics Center, Évora, Portugal, Chap. 6, pp. 147–169.
[36] Gosman, D. A., Pun, W. M., Runchal, A. K., Spalding, D. B., and Wolfsthein, C. M., 1969, *Heat and Mass Transfer in Recirculating Flows*, Academic, New York.
[37] Slattery, J. C., 1999, *Advanced Transport Phenomena*, Cambridge University Press, New York, pp. 50; 279–281.
[38] Davis, S. N., and DeWiest, R. J. M., 1966, *Hydrogeology*, Wiley, New York, p. 197.
[39] Bear, J., 1979, *Hydraulics of Groundwater*, McGraw-Hill, New York, p. 102.

V. A. F. Costa *is Associate Professor at the Universidade de Aveiro, Portugal. He received his M.Sc. and Ph.D. in Mechanical Engineering (heat transfer branch) from the University of Coimbra (Portugal) in 1989 and 1996, respectively. His main research and teaching activities include numerical heat transfer and fluid flow, convection heat transfer, engineering thermodynamics and drying. He uses several methods, including control volume finite element methods, with equal order interpolation for velocity and pressure. Some of recent work concerns the unification of the streamline, heatline, and massline methods, in order to have them ready to be treated in a common basis and ease to be implemented in CFD packages. He is author or co-author of 20 refereed archival papers in journals, and 30 papers in refereed conference proceedings in the aforementioned fields.*